THE JOURNAL OF PHYSICAL CHEMISTRY B

pubs.acs.org/JPCB Article

Site of Azido Substitution in the Sugar Moiety of Azidopyrimidine Nucleosides Influences the Reactivity of Aminyl Radicals Formed by Dissociative Electron Attachment

Mukesh Mudgal, Thao P. Dang, Adam J. Sobczak, Daniel A. Lumpuy, Priya Dutta, Samuel Ward, Katherine Ward, Moaadh Alahmadi, Anil Kumar, Michael D. Sevilla, Stanislaw F. Wnuk,* and Amitava Adhikary*

Cite This: https://dx.doi.org/10.1021/acs.jpcb.0c08201 Read Online

ABSTRACT: In this work, electron-induced site-specific formation of neutral π-type aminyl radicals (RNH·) and their reactions with pyrimidine nucleoside analogs azidolabeled at various positions in the sugar moiety, e.g., at 2′-, 3′-, 4′-, and 5′- sites along with a model compound 3-azido-1-propanol (3AZPrOH), were investigated. Electron paramagnetic resonance (EPR) studies confirmed the site and mechanism of RNH· formation via dissociative electron attachment-mediated loss of N_2 and subsequent facile protonation from the solvent employing the ^{15}N-labeled azido group, deuterations at specific sites in the sugar and base, and changing the solvent from H_2O to D_2O. Reactions of RNH· were investigated employing EPR by warming these samples from 77 K to ca. 170 K. RNH· at a primary carbon site (5′-azido-2′,5′-dideoxyuridine, 3AZPrOH) facilely converted to a σ-type iminyl radical (R=N·) via a bimolecular H-atom abstraction forming an α-azidoalkyl radical. RNH· when at a secondary carbon site (e.g., 2′-azido-2′-deoxyuridine) underwent bimolecular electrophilic addition to the C5=C6 double bond of a proximate pyrimidine base. Finally, RNH· at tertiary alkyl carbon (4′-azidocytidine) underwent little reaction. These results show the influence of the stereochemical and electronic environment on RNH· reactivity and allow the selection of those azidonucleosides that would be most effective in augmenting cellular radiation damage.

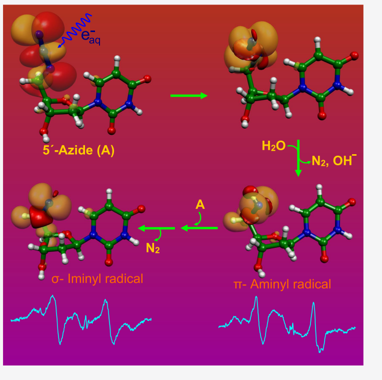

INTRODUCTION

Neutral aminyl radicals (RNH·) are π-type radicals that are important in chemical synthesis and in biology.[1−6] RNH· plays an important role in the prototropic equilibria of DNA-base π-cation radicals (such as guanine cation radical ($G^{\cdot+}$), cytosine cation radical ($C^{\cdot+}$), adenine cation radical ($A^{\cdot+}$)) that are involved in charge (hole) transfer processes followed by localization of damage.[4,6] Moreover, ·OH addition to the C4=C5 double bond in purine bases (G, A) followed by water elimination lead to the same RNH· species (G(N1−H)·, A(N6−H)·) that are formed via deprotonation of $G^{\cdot+}$ and $A^{\cdot+}$.[4,6] It is well established that RNH· undergo a wide variety of reactions that are summarized below.

(A) *Tautomerization*: π-Type RNH· is shown to undergo tautomerization to the σ-type R=N·:

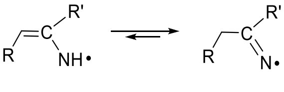

(1)

For example, electron paramagnetic resonance (EPR) studies have established that π-type aminyl radical (U-(5-C=CH_2)-NH·) formed from 5-(1-azidovinyl) modified 2′-deoxyuridine facilely tautomerizes to the σ-type iminyl radical, U-(5-C-CH_3)=N· (reaction 1a).[7]

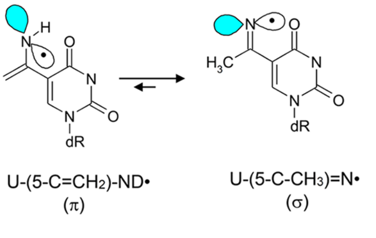

(1a)

Also, the deprotonated cytosine π-cation radical (C(N4−H)·) tautomerizes facilely to the σ-iminyl radical (reaction 1b).[17]

Received: September 8, 2020
Revised: November 9, 2020

Table 1. Hyperfine Coupling Constants (HFCC) and *g* Values of Radicals Reported in This Work

compound/type/radical	hyperfine couplings (G) site(nucleus)	exp	theory	*g* value (exp)
π/T(5′-CH_2)-NH·[a] (5′-AZT)	β-protons (H5′, H5″)	Sum 91[a]		
	N5′–H (α-proton)	(−, −, −30)[a]	(−39.8, 0.4, −26.7)[a]	$g_{\parallel}$ = 2.0020[a], $g_{\perp}$ = 2.0043[a]
	N5′-coupling	(0, 0, 43)[a]	(0, 0, 41.8) G [a]	
π/U-5-CH_2-NH·[b] (AmdU)	β-protons (H5, H5)[b]	Sum 93.5[b]		
5/π/dU-5′-CH_2-NH·	β-protons (H5′, H5″) (for **5**)	Sum 90.5		$g_{\parallel}$ = 2.0020, $g_{\perp}$ = 2.0043
	N5–H (α-proton)[b]	(−, −, −30)[a]		
	N5′–H (α-proton)			
	N5/N5′-coupling	(0, 0, 42.5)		
α-azidoalkyl radical	1αH		(−10.97, −15.03,-5.09)	2.0038 *yy*
5/π/dU-5′-CH·-N_3	1αH		(−14.46,-20.64,-6.67)	2.0021 *zz*
	1N		(10.5, −0.5, −1.32)[c]	2.0043 *xx*
σ U-5-CH═N·[b]	β-proton (H5) b	82[b]	(71.8, 78.0,72.8)	
	N5-coupling b	(0, 0, 36.5)[b]	(−4.2, 0, 37.7)[b]	$g_{\parallel}$ = 2.0016, $g_{\perp}$ = 2.0040
5 σ dR-5′-CH═N·	β-proton (H5′) **5**	82	(72.9, 78.7, 73.0)[d]	
	N5′-coupling	(0, 0, 36.5)	(−4.44, −0.9, 36.6)[d]	
1 π dC(C2′)-ND· (π C(C2′)-ND·)	N2′-coupling	(0, 0, 40.5)		
2 π dU(C2′)-ND· (π U(C2′)-ND·)	C2′–H (β-proton)	51.5		$g_{\parallel}$ = 2.0020, $g_{\perp}$ = 2.0043
	N2′–H (α-proton)	(*, *, −28)[e]		
3 π 2′,3′-ddU(C3′)-ND·	N3′-coupling	(0, 0, 37.5)[e]		$g_{\parallel}$ = 2.0020, $g_{\perp}$ = 2.0043
	C3′–H (β-proton)	41[e]		
	N3′–H (α-proton)	(*, *, −28)[e]		
4 π C(C4′)-ND·	N4′-coupling	(0, 0, 37.5)[e]		$g_{\parallel}$ = 2.0020, $g_{\perp}$ = 2.0043
	N4′–H (α-proton)	(*, *, −28)[e]		

[a]Taken from ref 8. [b]Taken from ref 7. [c]Employing the B3LYP/6-31G** method, the structure of 5′-CH·-N_3 was optimized and HFCCs of the fully optimized structure of 5′-CH·-N_3 was calculated (see the Supporting Information). Linewidth = 3.5 G and a mixed lineshape (Lorentzian/Gaussian = 1) was employed to simulate the experimental spectrum. [d]Employing the B3LYP/6-31G** method, structures of 5′-CH═N· of U-5-CH═N· were fully optimized and HFCCs of these optimized structures were calculated (see the Supporting Information). Linewidths as (7, 5, 5) G and lineshape with a mixed Lorentzian/Gaussian = 1 were employed to simulate the experimental spectrum. [e]Taken from ref 8. For simulation, we used linewidth = 10 G and lineshape with a mixed Lorentzian/Gaussian = 1.

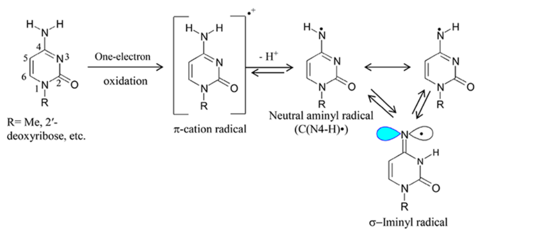

(1b)

(B) *Intermolecular H-atom abstraction generating C-centered radicals*: It is well established that RNH· can abstract H atoms from weaker CX–H bonds via a bimolecular pathway to form C-centered radicals.[1−16] For example, RNH· generated from AZT undergo bimolecular H-atom abstractions from the $-CH_3$ group at C5 of thymine base forming the allylic radical, $dUCH_2$· (ca. 55%), and from the C5′-site of a proximate AZT producing the strand break precursor radical, C5′·.[8]

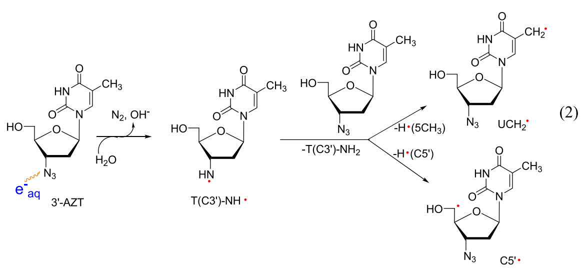

(2)

In addition, intermolecular H-atom abstraction by RNH· from a proximate compound (e.g., 5-azidomethyl-2′-deoxyuridine) having an α-azidoalkyl moiety leads to the formation of an α-azidoalkyl radical, which undergoes a facile conversion to the σ-type R′═N·:[7]

$$\mathrm{RNH\cdot} \xrightarrow[-\,\mathrm{RNH_2}]{\mathrm{R'-CH_2-N_3}} \mathrm{R'-\dot{C}H-N_3} \xrightarrow{-\mathrm{N_2}} \mathrm{R'-CH{=}N\cdot} \quad (2a)$$

(C) Transposition of radical site via intramolecular H-atom transfer, e.g., 1,2 shift, 1,5 shift: Pulse radiolysis of amino acids at ambient temperature presented evidence of 1,2 H-atom shift in the ·OH-mediated formation of oxidizing radicals in amino acids, for example, aminyl radical (·NH–CH_2–CO_2^-) from glycine rearranges to NH–·CH_2–CO_2^- by intramolecular 1,2 H-shift (reaction 3):[22,23]

$$\mathrm{\cdot NH-CH_2-CO_2^-} \xrightarrow[\text{shift}]{\text{1,2 H-atom}} \mathrm{NH_2-\dot{C}H-CO_2^-} \quad (3)$$

EPR studies have presented evidence of facile and intramolecular 1,5 H-shift in RNH· in lyxofuranoside leading to the formation of C5· radical.[9]

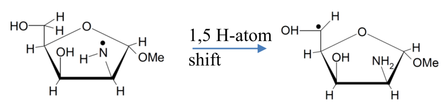

(3a)

(D) *β-Elimination*: Pulse radiolysis has shown that the oxidizing aminyl radical (e.g., ·NH–CH_2–CO_2^-) generated by the reaction of ·OH with an amino acid (e.g., glycine) leads to the formation of CO_2·⁻ (reaction 4):[22,23]

$$\mathrm{\cdot NH-CH_2-CO_2^-} \rightarrow \mathrm{NH{=}CH_2} + \mathrm{CO_2^{\bullet -}} \quad (4)$$

https://dx.doi.org/10.1021/acs.jpcb.0c08201
J. Phys. Chem. B XXXX, XXX, XXX−XXX

Scheme 1. Synthesis of 2′-Azido-2′-deoxyuridine 2 and Its 5,6-[$^2H_2$]-2 and 2′-[^{15}N]-N_3-2 Isotopes

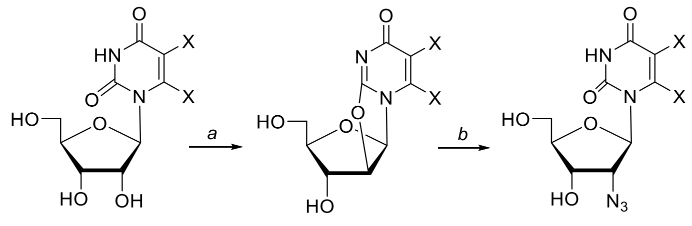

8a X = H
8b X = D

9a X = H
9b X = D

2 X = H
5,6-[$^2H_2$]-**2** X = D
2′-[^{15}N]-N_3-**2** X = H

Reagents: (*a*) $(PhO)_2CO/NaHCO_3$/DMF; (*b*) NaN_3 or [^{15}N]-NaN_3/BzOH/HMPA

(E) *Intramolecular cyclization*: Dialkylaminyl radicals [R═H, Me; R′═H, Me (reaction 5)] are shown to undergo intramolecular cyclization reactions leading to the formation of C-centered radicals.[10,16]

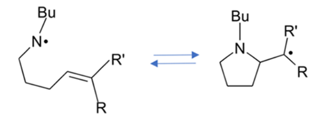

(5)

RNH· radical is generated by one-electron oxidation of primary amines followed by deprotonation of the primary amine cation radical ($RNH_2^{\cdot+}$).[4,17−34] Thus, RNH· becomes the Brønsted base, $RNH_2^{\cdot+}$ is the conjugate acid, and these two species (RNH· and $RNH_2^{\cdot+}$) are in prototropic equilibrium if R is a delocalized structure (see for example, reaction 1b). In addition, the formation of RNH· via photodissociation[11−15] and via ·OH employing pulse radiolysis[4,22,23] have been reported.

We have developed a novel method of site-specific electron-mediated RNH· generation employing azidonucleosides (reaction 2).[6−9] Our work has established that radiation-produced prehydrated electron (e_{pre}^-)-mediated dissociative electron attachment to azidonucleosides (RN_3) in homogeneous supercooled glassy systems at 77 K,[9] at first, leads to the formation of highly basic and unstable nitrene anion radical ($RN^{\cdot-}$) at 77 K via spontaneous loss of N_2 from the azidonucleoside anion radical ($RN_3^{\cdot-}$). Subsequent facile protonation of $RN^{\cdot-}$ produces RNH·. Neither $RN_3^{\cdot-}$ nor $RN^{\cdot-}$ intermediates were detected by using electron paramagnetic resonance (EPR) spectroscopy even at 77 K, and only the EPR spectra of RNH· were observed.[6−9] So far, investigations from our laboratory have presented evidence of reactions 1−3a. Also, our work has shown that reaction mechanisms of RNH· depend on the type of compounds (azidomethyl vs azidovinyl)[6,7] and conformation of the sugar (lyxofuranose vs 2′-deoxyribofuranose).[9]

In this work, we have employed uracil and cytosine nucleosides with the azido group substituted at the 2′ (2′-azido-2′-deoxycytidine (2′-AZdC, **1**), 2′-azido-2′-deoxyuridine (2′-AZdU, **2**)), 3′ (3′-azido-2′,3′-ddU, **3**)); 4′ (4′-azidocytidine (4′-AZC, **4**)); and 5′ (5′-azido-2′,5′-dideoxyuridine (5′-AZ-2′,5′-ddU, **5**), 5′-azido-5′-deoxythymidine (5′-AZT, **6**)) positions. An azido-substituted alcohol (3-azido-1-propanol (3AZPrOH, **7**)) has also been investigated as a model of azido group linked to the primary carbon. Thus, the azido group is attached to the primary carbon, 5′ (**5**, **6**) and 3AZPrOH (**7**), to the secondary carbon (2′ and 3′), and to the tertiary carbon (4′) site. RNH· formation via attachment of radiation-produced prehydrated electrons to these compounds in γ-irradiated aqueous glassy (7.5 M LiCl) systems and subsequent reactions of RNH· are investigated employing EPR spectroscopy. A set of [^2H]-labeled **2** (C2′, C3′, C4′, C5, and C6) isotopomers and that of [^{15}N]-azido labeled **2** have led us to unambiguously assign that in all compounds including the isotopically substituted ones, the predominant site of electron attachment is the azido group, and to characterize the resultant RNH· and its subsequent reactions. The experimentally obtained hyperfine coupling constant (HFCC) values of RNH· have been compared with the corresponding theoretically calculated values for EPR spectral assignment (Table 1). Similar to our earlier work on the reaction of RNH· from the azido substitution to a primary carbon at C5 of 5-azidomethyl-2′-deoxyuridine (AmdU),[7] a bimolecular conversion of RNH· attached to a primary carbon site (5′, **5**, **6**) to the σ-type iminyl radical (R═N·) involving an α-azidoalkyl radical as intermediate was observed. RNH· from **7** underwent this conversion as well. Thus, our earlier results from AmdU,[7] our results from **5**, **6**, and **7** in this worked have established the general nature of this RNH· to R═N· bimolecular conversion, i.e., this conversion happens in any azido compound in which the azido group is linked to a primary carbon. Bimolecular electrophilic addition of RNH· attached to the secondary carbon site to the C5═C6 double bond of a proximate pyrimidine (uracil and cytosine but not thymine) base is observed. Finally, a little reaction was observed in the glassy system from RNH· at tertiary alkyl carbon. Our results presented in this work demonstrate that the stereochemical and electronic environment of azido substitution at specific sites in the sugar moiety significantly affect the reactivity of RNH·. Azidonucleosides have also been shown to augment radiation damage in various types of cancer cells.[7,35−39] In addition, 2′-azido-2′-deoxyuridine (**2**) 5′-phosphate is shown to be a potent inhibitor of ribonucleotide reductases following a radical chemistry-based inactivation pathway.[40−42] Therefore, the results presented in this work in conjunction with our own work on azido substitution at C5 in the pyrimidine base[7] provide the basis to choose the type of azidonucleoside that will be suitable to augment significant radiation damage to tumor cells, thereby improving the efficacy of tumor radiochemotherapy.

■ EXPERIMENTAL SECTION

2′-Azido-2′-deoxycytidine (2′-AZdC, **1**)[43] and 4′-azidocytidine (4′-AZC, **4**)[44] were prepared by slight modifications of the literature protocols. The synthesis and spectroscopic characterization of 2′-azido-2′-deoxyuridine (2′-AZdU, **2**) and its derivatives with deuterations at specific sites of the sugar moiety, e.g., 2′-D-2′-AZdU ([**2′-D**]-**2**), 3′-D-2′-AZdU ([**3′-D**]-**2**), and 4′-D-2′-AZdU ([**4′-D**]-**2**), or at the base, 5,6-D,D-2′-

AZdU ([**5,6-D,D**]-**2**) and ^{15}N incorporated azido group in **2** are described in the main manuscript (Schemes 1 and 2). The general experimental methodologies and synthesis of all other synthetic intermediates (Schemes S1 and S2) are described in the Supporting Information. Azido compounds 3′-AZ-2′,3′-ddU (**3**), 5′-AZ-2′,5′-ddU (**5**), 5′-AZT (**6**), 3AZPrOH (**7**), and 3′-AZT are commercially available. Sodium azide ^{15}N-labeled (97%) in the terminal position and deuterium-labeled uracil were purchased from Cambridge Isotope Laboratories.

Scheme 2. Synthesis of Ribose Deuterated 2′-Azido-2′-deoxyuridine isotopes 2′-[^{2}H]-2 (X = D), 3′-[^{2}H]-2 (Y = D), and 4′-[^{2}H]-2 (Z = D)

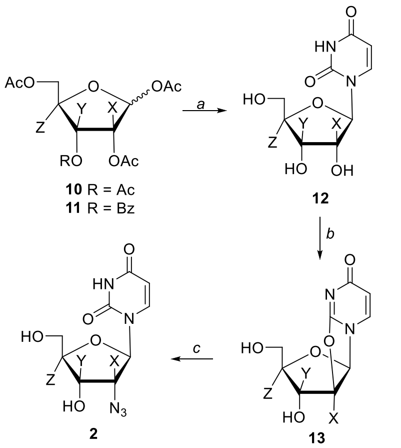

For compounds **10-13** X = Y = Z = H, except
Series: **a**, X = D; **b**, Y = D; **c**, Z = D

Reagents: (*a*) (i) uracil/HMDS/TMSSiCl, (ii) TMSOTf/MeCN, (iii) NH_3/MeOH; (*b*) $(PhO)_2CO/NaHCO_3$/DMF; (*c*) NaN_3/BzOH/HMPA

For EPR studies, methods of preparation of homogeneous glassy samples of **1** to **7**, [**2′-D**]-**2**, [**3′-D**]-**2**), [**4′-D**]-**2**), [**5,6-D,D**]-**2**, and ^{15}N incorporated azido group in **2** in 7.5 M LiCl/D_2O or 7.5 M LiCl/H_2O, γ-irradiation and storage of these glassy samples including the stepwise annealing of these glassy samples are described in the Supporting Information. An EPR spectrometer, experimental setup (field calibration employing Fremy's salt, microwave power, etc.) for recording the EPR spectra at 77 K, and methods of theoretical calculations are described in the Supporting Information.

■ RESULTS

Synthesis. The 2′-azido-2′-deoxyuridine **2** (2′-AZdU) and its selectively labeled 5,6-[$^2H_2$]-**2**, , 2′-[^{2}H]-**2**, 3′-[^{2}H]-**2**, and 4′-[^{2}H]-**2** analogues were prepared by conversion of uridine **8a** and the selectively deuterated uridine analogues **8b** and **12a**−**c** to 2,2′-*O*-anhydrouridine derivatives **9a**, **9b**, and **13a**−**c** employing the Hampton and Nichol methodology.[45] Subsequent ring-opening with azide anion [generated from trimethylsilylazide ($TMSN_3$)/LiF and tetramethylethylenediamine (TMEDA) or NaN_3 in hexamethylphosphoramide (HMPA) in the presence of benzoic acid] gave desired 2′-azido-2′-deoxyuridine **2**[46,47] and its deuterium-labeled analogues in uracil 5,6-[$^2H_2$]-**2** (Scheme 1) or ribose (2′-[^{2}H]-**2**, 3′-[^{2}H]-**2**, and 4′-[^{2}H]-**2**; Scheme 2) moieties. Ring-opening of **9a** with [^{15}N]-NaN_3 provided 2′-[^{15}N]-azido-labeled **2** (Scheme 1).[48] The selectively deuterated ribofuranose precursors 2-[^{2}H]-**10a**, 3-[^{2}H]-**10b** (Schemes S1 and S2), and 4-[^{2}H]-**11c** were prepared following literature methodologies, and the details of their synthesis as well as their coupling with uracil to give uridines **12a**−**c**; their subsequent conversion to 2,2′-*O*-anhydro precursors **13a**−**c** are described in the Supporting Information.

*2′-Azido-2′-deoxyuridine (**2**).* The stirred solution of **9a** (30 mg, 0.13 mmol; see the Supporting Information for the preparation of **9a**) and NaN_3 (60 mg, 0.93 mmol) in HMPA (0.5 mL) was heated at 150 °C. After 30 min, benzoic acid (16 mg, 0.13 mmol) was added and heating was continued for another 15 min. The cooled reaction mixture was diluted with H_2O and washed with $CHCl_3$. The organic layer was back-extracted with H_2O. The combined aqueous layers was concentrated and purified on silica gel column (EtOAc/MeOH, 9:1) or preparative RP-HPLC (H_2O/MeCN, 6:1) to afford **2**[46,47] (20 mg, 56%): ^{1}H NMR (D_2O) δ 3.70 (dd, J = 4.3, 12.8 Hz, 1, H5″), 3.82 (dd, J = 2.8, 12.8 Hz, 1, H5′), 4.00 ("ddd", J = 2.9, 4.2, 6.0 Hz, 1, H4′), 4.22 ("dd", J = 4.5, 5.7 Hz, 1, H2′), 4.35 (t, J = 5.9 Hz, 1, H3′), 5.77 (d, J = 8.1 Hz, 1, H5), 5.80 (d, J = 4.4 Hz, 1, H1′), 7.75 (d, J = 8.1 Hz, 1, H6); MS (ESI$^-$) m/z 268 (MH$^-$).

*2′-[^{15}N]-N_3-2′-Azido-2′-deoxyuridine (2′-[^{15}N]-N_3-**2**).* Treatment of **9a** (20 mg, 0.09 mmol) with [^{15}N]-NaN_3 (40.5 mg, 0.61 mmol; >97% ^{15}N) as described above gave 2′-[^{15}N]-N_3-**2**[48] (8 mg, 33%) with identical physical, chemical, and spectroscopic properties (^{1}H NMR) as **2** except for MS (ESI$^-$) m/z 269 (M − H$^-$).

*5,6-[$^2H_2$]-2′-Azido-2′-deoxyuridine (5,6-[$^2H_2$]-**2**).* Azidation of **9b** (18 mg, 0.08 mmol; see the Supporting Information for the preparation of **9b**) as described above afforded 5,6-[$^2H_2$]-**2** (11 mg, 52%) with identical physical, chemical, and spectroscopic properties as **2** except for the disappearance of H6 peak at 7.75 ppm and the presence of the residual peak (∼ 30%) for H5 at 5.77 ppm (s): MS (ESI$^-$) m/z 270 (MH$^-$).

*2′-[^{2}H]-2′-Azido-2′-deoxyuridine (2′-[^{2}H]-**2**).* Azidation of **13a** (22 mg, 0.10 mmol) as described above afforded 2′-[^{2}H]-**2** (7 mg, 27%) with identical spectroscopic properties as **2** except for the disappearance of H2′ at 4.22 ppm and simplification of proton splitting for H1′ at 5.80 ppm (s) and H3′ at 4.35 ppm (d, J = 6.0 Hz); MS (ESI$^-$) m/z 269 (MH$^-$).

*3′-[^{2}H]-2′-Azido-2′-Deoxyuridine (3′-[^{2}H]-**2**).* Azidation of **13b** (20 mg, 0.09 mmol) as described above afforded 3′-[^{2}H]-**2** (15 mg, 63%) with identical spectroscopic properties as **2** except for the disappearance of the H3′ peak at 4.35 ppm and simplification of proton splitting for H2′ at 4.22 ppm (d, J = 4.5 Hz) and H4′ at 4.00 ppm ("dd", J = 2.9, 4.2 Hz): MS (ESI$^-$) m/z 269 (MH$^-$).

*4′-[^{2}H]-2′-Azido-2′-deoxyuridine (4′-[^{2}H]-**2**).* Azidation of **13c** (25 mg, 0.11 mmol) as described above afforded 4′-[^{2}H]-**2** (20 mg, 67%) with identical spectroscopic properties as **2** except for the disappearance of the H4′ peak at 4.00 ppm and simplification of proton splitting for H3′ at 4.35 ppm (d, J = 5.8 Hz), H5′ at 3.82 ppm (d, J = 12.8 Hz), and H5″ at 3.70 ppm (d, J = 12.8 Hz): MS (ESI$^-$) m/z 269 (MH$^-$).

EPR Studies. *Characterization of RNH·.* Characterization of the RNH· formed from glassy samples of 2′-azido-2′-deoxyuridine (2′-AZdU, **2**) is presented here as an example. From our previous assignments of RNH·[6−9] (for example, T(C2′)-^{14}ND· in 3′-AZT[8]) the major HFCC values in RNH· from **2** (dU(C2′)-^{14}ND· and its corresponding ^{15}ND· analog (dU(C2′)-^{15}ND·)) are expected from three sources: the axially symmetric anisotropic HFCC from the azide N, the isotropic β-proton coupling owing to H2′, and the αH/aD anisotropic hyperfine coupling from the exchangeable NH/ND.

https://dx.doi.org/10.1021/acs.jpcb.0c08201
J. Phys. Chem. B XXXX, XXX, XXX−XXX

Assignment of the Axially Symmetric Anisotropic HFCC Due to the Aminyl N. The 77 K EPR spectrum (green) of RNH· (U(C2′)-^{14}ND·) formed via γ-radiation-induced (absorbed dose = 500 Gy at 77 K) electron attachment in an aqueous glassy (7.5 M LiCl/D_2O (pH ca. 5)) sample of **2** (1 mg/mL) after visible illumination by using a photoflood lamp at 77 K for 15 min is presented in Figure 1A. The 77 K visible illumination was carried out following our work on T(C2′)-^{14}ND·) in 3′-AZT[8]; 77 K visible illumination removed line components of uracil anion radical by photoejection of the excess electron. The spectrum in Figure 1A shows a large central doublet due to an isotropic β-proton HFCC value of H2′ at 51.5 G, a triplet from an axially symmetric anisotropic aminyl ^{14}N (spin = 1) HFCC (A_{zz} ($A_{\parallel}$) = 40.5 G, $A_{\perp} = A_{xx} = A_{yy}$ = 0 G), along with $g_{\parallel}$ = 2.0020 and $g_{\perp}$ = 2.0043 (see also Figure 2A and Table 1). The anisotropic ^{14}N HFCC and the g values agree with those of aminyl radicals reported in the literature.[7−9,17−29] Based on these results, the green spectrum in Figure 1A is assigned to U(C2′)-^{14}ND·.

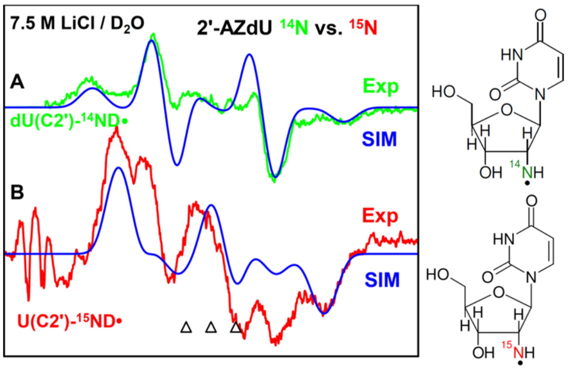

Figure 1. 77 K EPR spectrum of RNH· (U(C2′)-^{14}ND·) formed via electron-induced attachment in an aqueous glassy (7.5 M LiCl/D_2O) sample of (A) unlabeled **2**, green color, and (B) ^{15}N labeled **2**, red color, after visible illumination of each sample by using a photoflood lamp at 77 K for 15 min to remove the uracil anion radical by photoejection of the excess electron. The simulated spectra (blue) (for simulation parameters, see text) are superimposed on the top of the each experimentally recorded spectrum. The three reference markers (open triangles) in this figure and in other figures show the position of Fremy's salt resonance with the central marker at g = 2.0056. Each of these markers is separated from each other by 13.09 G.

Based on our previous work on 1-Me-(C2)-^{15}ND· from methyl 2-azido-2-deoxy-β-D-ribofuranoside,[9] experiments were carried out using a matched sample of ^{15}N incorporated **2** (where the N atoms in the 2′-azido group of **2** were ^{15}N labeled) to make this assignment of U(C2′)-^{14}ND· unequivocal; the results are presented in Figure 1B. Analyses of the experimentally recorded spectrum (red) in Figure 1B shows the large central doublet due to an isotropic β-proton HFCC value of H2′ at 51.5 G and $g_{\parallel}$ = 2.0020 and $g_{\perp}$ = 2.0043 (same as the green spectrum in Figure 1A). The red spectrum in Figure 1B also shows line components due to an axially symmetric anisotropic aminyl ^{15}N (spin = 1/2) HFCC (A_{zz} = 56.9 G, $A_{xx} = A_{yy}$ = 0 G). Following our assignment of the green spectrum in Figure 1A to U(C2′)-^{14}ND·, the red spectrum in Figure 1B is assigned to U(C2′)-^{15}ND·. ^{15}N (spin = 1/2) couplings are found to be 1.404 times the ^{14}N (spin = 1), and this is equal to the gyromagnetic ratio of ^{15}N/^{14}N.[9,18] We note here that each experimentally recorded spectrum shown in Figure 1A,B was obtained after subtraction of the line components of the $Cl_2^{\cdot-}$ spectrum following our previous works on the isolation of the 77 K RNH· spectrum.[7−9,49−51] A small residual peak of the $Cl_2^{\cdot-}$ subtraction is found on the low field end of the red spectrum in Figure 1B. This does not belong to the experimental U(C2′)-^{15}ND· spectrum (red). Employing these HFCC and g values, the U(C2′)-^{14}ND· (green, Figure 1A) spectrum and U(C2′)-^{15}ND· (red, Figure 1B) spectrum were simulated employing the following parameters: anisotropic α-D (N-D) HFCC (4.5, 0, 6) G[7−9] and a mixed Lorentzian/Gaussian (1/1) linewidth of 10 G. The simulated spectra (blue) matched nicely with corresponding experimentally recorded spectra in Figure 1A,B. These results provided unequivocal assignment of the axially symmetric anisotropic N HFCC of RNH·.

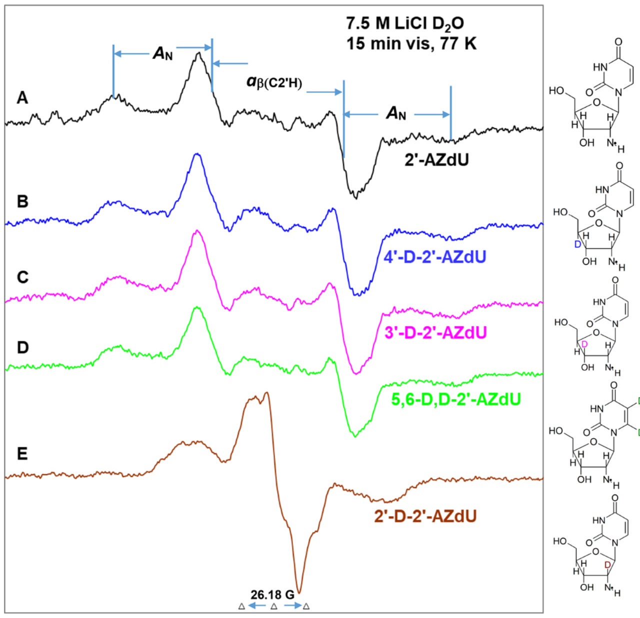

Figure 2. EPR spectra of the aminyl radicals (dU(C2′)-ND·) found in matched samples (1 mg/mL of each compound) via radiation-produced (absorbed dose = 500 Gy at 77 K) one-electron addition at 77 K of the homogeneous glassy solution of 7.5 M LiCl in D_2O after visible illumination of each sample by using a photoflood lamp at 77 K for 15 min to remove the uracil anion radical by photoejection of the excess electron of (A) 2′-AZdU (**2**), (B) 4′-D-2′-AZdU ([**4′-D**]-**2**), (C) 3′-D-2′-AZdU ([**3′-D**]-**2**), (D) 5,6-D,D-2′-AZdU ([**5,6-D,D**]-**2**), and (E) 2′-D-2′-AZdU ([**2′-D**]-**2**). The extent of β-hyperfine coupling by H2′ atom and the anisotropic nitrogen hyperfine coupling $A_{\parallel}$ in U(C2′)-ND· of 2′-AZdU are represented by stick diagrams.

Sugar Deuteration Studies Establish That the Isotropic β-Hydrogen HFCC in dU(C2′)-ND· Originates from H2′. To investigate the origin of β-hydrogen coupling, we have employed matched homogeneous glassy samples (1 mg/ mL of each compound) of **2** and its derivatives with deuterium substitution at specific sites in the deoxyribose sugar (at 2′ ([**2′-D**]-**2**), 3′ ([**3′-D**]-**2**), and 4′ ([**4′-D**]-**2**)) and at the C5,C6 sites of uracil base moiety ([**5,6-D,D**]-**2**)). EPR spectra of dU(C2′)-ND· formed in these samples via γ-radiation-induced (absorbed dose ca. 500 Gy at 77 K) electron attachment after visible illumination by using a photoflood lamp at 77 K for 15 min are shown in Figure 2. Each experimentally recorded spectrum shown in Figure 2 was obtained after subtraction of the line components of the $Cl_2^{\cdot-}$ spectrum following our previous works on the isolation of the 77 K RNH spectrum.[7−9,49−51] Analyses of the spectra presented in Figure 2A−E establish that the EPR spectrum of dU(C2′)-ND· is affected only by deuteration at 2′

https://dx.doi.org/10.1021/acs.jpcb.0c08201
J. Phys. Chem. B XXXX, XXX, XXX−XXX

(spectrum in Figure 2E). The total hyperfine splitting, lineshape, and center of the spectra remain unchanged in spectra presented in Figure 2A−D. Following our analyses of the green spectrum in Figure 1A, spectra presented in Figure 2 show a large central doublet due to an isotropic β-proton HFCC value of H2′ at 51.5 G, a triplet from an axially symmetric anisotropic aminyl N HFCC (A_{zz} ($A_{\parallel}$) = 40.5 G, $A_{\perp} = A_{xx} = A_{yy}$ = 0 G), along with $g_{\parallel}$ = 2.0020 and $g_{\perp}$ = 2.0043.

The collapse of the ca. 51.5 G doublet due to deuteration at 2′ ([**2′-D**]-**2**) in the spectrum in Figure 2E establishes unequivocally the presence of β-H2′ HFCC in dU(C2′)-ND·. All other analogs of **2** having deuteration at the C5 and C6 positions in the uracil ring or at positions other than C2′ in the sugar moiety show this doublet in the dU(C2′)-ND· spectrum.

Studies in D_2O vs H_2O Establish the αH-Atom Anisotropic Hyperfine Coupling of the Exchangeable N−H Proton in dU(C2′)-ND· (or dU(C2′)-NH·). EPR spectral studies of radiation-produced electron attachment to matched samples of **2** in H_2O glasses (7.5 M LiCl/H_2O) were performed and compared with the results obtained in D_2O glasses (7.5 M LiCl/D_2O, Figure 1).

These results are shown in Figure 3 below. Comparison of the linewidth of the green-colored spectrum (in D_2O) shown in Figure 3A with that of the red-colored spectrum (in H_2O, Figure 3B) clearly establishes that the central doublet observed in the red-colored spectrum in Figure 3B is due to an extra proton hyperfine coupling in the aminyl radical in H_2O (U(C2′)-NH·) that is present in the H_2O glasses and is missing in the D_2O glasses (dU(C2′)-ND·, green color) as it is an exchangeable proton. Comparison of these two spectra clearly shows the $A_{\parallel}$ (i.e., the A_{zz}) component ca. 22 G due to the α-N−H proton of the aminyl radical in H_2O (U(C2′)-NH·) (red color) is lost in the D_2O glasses (green color) because a deuteron coupling is only 15% (1/6.514) that of a proton in the same environment.

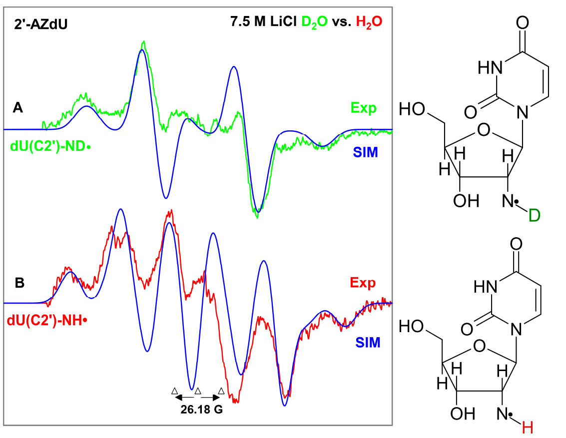

Figure 3. EPR spectrum of aminyl radical formed in matched samples (1 mg/mL of each compound) via radiation-produced (absorbed dose = 500 Gy at 77 K) one-electron addition by γ-irradiation of **2** (A) dU(C2′)-ND· (green color) in 7.5 M LiCl (D_2O) and (B) dU(C2′)-NH· (red color) in 7.5 M LiCl (H_2O) color after visible illumination of each sample by using a photoflood lamp at 77 K for 15 min to remove the uracil anion radical by photoejection of the excess electron. Panel (A) is the same one shown in Figures 1A and 2A. The simulated spectra (blue) are superimposed on the top of the experimentally recorded spectra for comparison. Each experimentally recorded spectrum shown in Figure 2 was obtained after subtraction of the line components of the $Cl_2^{\cdot-}$ spectrum following our previous works on the isolation of the 77 K RNH· spectrum.[7−9,49−51]

Therefore, the results presented in Figures 1−3 clearly establish the electron-induced site-specific formation of π-RND·/π-RNH· (dU(C2′)-ND·)/dU(C2′)-NH·) from **2** and its various deuterated derivatives [**2′-D**]-**2**, [**3′-D**]-**2**, [**4′-D**]-**2**, and [**5,6-D,D**]-**2** (Scheme 3). These results further confirm that the

Scheme 3. Radiation-Produced Electron-Mediated Site-Specific Formation of dU(C2′)-NH· from 2[a]

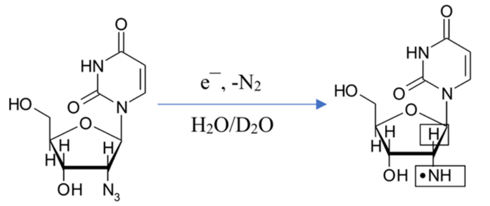

2 dU(C2')-NH•

[a]Boxes in the structure of dU(C2′)-ND· indicate those nuclei with substantial HFCC values. These couplings arise from the axially symmetric anisotropic azide N, the isotropic β-proton (H2′), and the anisotropic αH/αD of the exchangeable NH/ND.

HFCC values due to the axially symmetric anisotropic ^{14}N, the isotropic β-proton (H2′), and the anisotropic αH/αD of the exchangeable NH/ND contribute to the total hyperfine splitting of dU(C2′)-ND·.

We note here that these results, along with our previous results on radiation-produced prehydrated electron-mediated formation of RNH· and their reactions in 5-azidopyrimidines,[7] AZT derivatives,[8] and azidopentoses,[9] reported predominant formation of phenylnitrene anion radical due to gas-phase low-energy electron (LEE, 0 to 1 eV) attachment to phenylazide.[8,52,53] Light-induced reduction of aromatic azides to amines in the presence of CdS and CdSe nanoparticles[8,54] showed the facile and site-specific formation of RNH· from a localized $RN_3^{\cdot-}$ (Scheme 3). In addition, pulse radiolysis carried out in aqueous solution of 3′-AZT at ambient temperature reports that the solvated (aqueous) electron reacts with 3′-AZT with a diffusion-controlled rate ($k = 1.9 \times 10^{10}$ M^{-1} s^{-1}),[55] thereby supporting the reaction mechanism and its facile nature represented in Scheme 3.

*Reactions of Aminyl Radicals. RNH· Formed at a Primary Carbon Site (5′-Azido-2′,5′-dideoxyuridine (5′-AZ-2′,5′-ddU, **5**)) Converts Bimolecularly to the σ-Type Iminyl Radical (R═N·) Involving an α-Azidoalkyl Radical Intermediate.* Figure 4 presents the EPR spectra (red) showing the formation of RNH· by prehydrated electron attachment[7−9,50] to **5** (5 mg/mL) and the subsequent reactions of RNH· in supercooled homogeneous glassy (7.5 M LiCl/D_2O) solutions. Electrons were produced by gamma radiation (absorbed dose = 500 Gy at 77 K). These spectra are overlapped on our recently published spectra (blue) of radiation-produced electron-induced formation of π-type RNH· and its reactions in 5-azidomethyl 2′-deoxyuridine (AmdU) samples.[7] Note that all the EPR spectra presented in Figure 4 and in subsequent figures are obtained after subtraction of line components due to the expected low-field resonance from the matrix radical, $Cl_2^{\cdot-}$, which are produced by scavenging of radiation-produced holes (reactions 6 and 7).[7−9,49−51]

$$h^+ + Cl^- \rightarrow Cl\cdot \quad (6)$$

$$Cl\cdot + Cl^- \rightarrow Cl_2^{\cdot-} \quad (7)$$

https://dx.doi.org/10.1021/acs.jpcb.0c08201
J. Phys. Chem. B XXXX, XXX, XXX−XXX

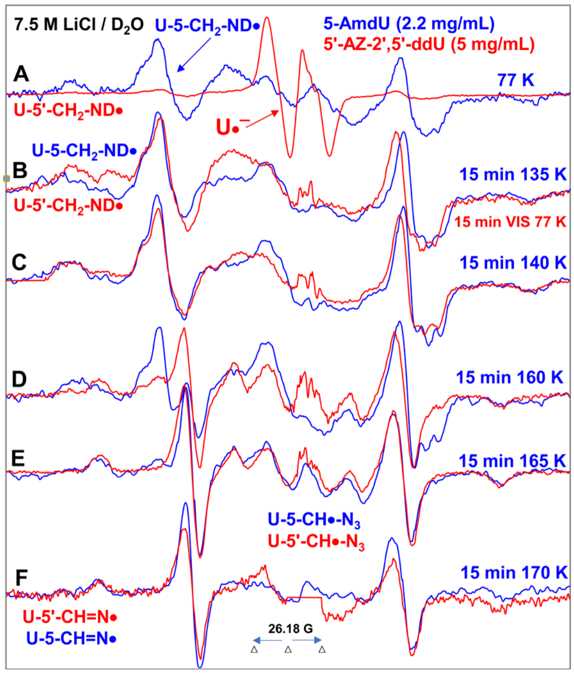

Figure 4. Spectra (A−D) in red were obtained from samples of 5′-AZ-2′,5′-ddU (**5**) ([**5**] = 5 mg/mL) after subtraction of the $Cl_2^{\cdot -}$ spectrum[7−9,49] from the individual experimentally recorded spectrum. (A) EPR spectrum (red) after radiation-produced prehydrated one-electron addition to the same sample of **5** at 77 K in 7.5 M LiCl/D_2O. Spectrum (B, red) was obtained after 15 min photoexcitation by a photoflood lamp at 77 K. Spectra (C, red) to (F, red) were obtained via stepwise annealing of the sample for 15 min at 140, 160, 165, and 170 K. All spectra were recorded at 77 K. Sum of two isotropic β-proton couplings is assigned to the central doublet (ca. 90.5 G) found in red spectra (A) to (D); the large central doublet (ca. 82 G) in spectra (D−F, red) is due to one isotropic β-proton coupling. Meanwhile, the wings in spectra (A)−(F) show the A_{zz} components of the anisotropic nitrogen hyperfine coupling. All spectra were recorded at 77 K. The experimental spectra from AmdU from ref 7 (2.2 mg/mL, blue) are superimposed in (A)−(F) for comparison.

Figure 4A presents the EPR spectrum (red) of the radicals formed in the sample of **5** at 77 K. The center of spectrum in Figure 4A shows the doublet[27−29] expected for U·−. Furthermore, a comparison of this red spectrum with the already reported spectrum (blue) of the neutral π-aminyl radical U-5-CH_2-ND· from AmdU samples at 77 K[7] shows that the red spectrum has additional line components that match nicely with those due to U-5-CH_2-ND·. Therefore, we assign these line components to the neutral π-aminyl radical U-5′-CH_2-ND· in the red spectrum in Figure 4A.

Following our work on AZT,[8] photoejection of the electron from the U·− via visible photoexcitation at 77 K results in the red spectrum shown in Figure 4B. Comparison of the red spectrum in Figure 4B with the corresponding one in Figure 4A shows that the central doublet due to U·− is absent in the red spectrum in Figure 4B. Therefore, we conclude that the electron has been completely photoejected from U·− to form U and has reacted with parent **5** to produce additional U-5′-CH_2-ND·. Total hyperfine splitting of the red spectra in Figure 4A,B is ca. 175.5 G (see Figure S1) in comparison to that (178.5 G) found in the blue spectra in Figure 4A,B. Moreover, the U-5′-CH_2-ND· spectrum (red, Figure 4B) from **5** is very similar to the reported spectrum[7] of U-5-CH_2-ND· (blue, Figure 4B) from AmdU obtained via annealing in the dark at ca. 135 K for 15 min. Thus, the hyperfine structures of the red spectrum in Figure 4B are due to a single axially symmetric anisotropic nitrogen with hyperfine coupling constant (HFCC) value as (42.5, 0, 0) G along with values of $g_{\parallel}$ (2.0020) and $g_{\perp}$ (2.0043) that are typical of a neutral aminyl radical nitrogen (Table 1). This is manifested by the excellent agreement of these N HFCC, $g_{\parallel}$, and $g_{\perp}$ values with the corresponding nitrogen HFCC, $g_{\parallel}$, and $g_{\perp}$ values of T(5′-CH_2)-NH· from 5′-AZT[8] and of U-5-CH_2-NH· from AmdU.[7]

The spectra (red, Figure 4A,B) of U-5′-CH_2-ND· show a broad doublet of ca. 90.5 G (see Figure S1), and this is very similar to the published spectra of (ca. 93.5 G) U-5-CH_2-NH· (blue, Figure 4A,B) from AmdU[7] and of (ca. 91 G) T(5′-CH_2)-NH· from 5′-AZT (**6**).[8] As for these similar structures, the radical-site *p* orbital on the aminyl-N at C5′-CH_2 in U-5′-CH_2-ND· strongly couples with two 5′-CH_2− protons that are attached to C5′ and gives rise to this broad doublet spectrum. These results show that substitution of the −CH_2−N_3 moiety either at the sugar of **5** or at the uracil base of AmdU[7] yields similar π-aminyl radical (U-5′-CH_2-ND· vs U-5-CH_2-ND·) with near-identical EPR spectra.

Taking the U·− spectrum from the literature[27−29] and the U-5′-CH_2-ND· spectrum (red, Figure 4B) as benchmarks, analysis of the red spectrum in Figure 4A shows that this spectrum is a cohort of spectra due to two radicals, i.e., U-5′-CH_2-ND· (ca. 80%) and U·− (ca. 20%). Thus, the predominant site of electron capture in azido compounds used in this work and in our previous works[6−9] is the azido group; thus, the azido group is even more electron affinic than uracil, the most electron affinic nucleic acid base. These results, in agreement with our previous results,[6−9] further establish the facile formation of site-specific neutral π-aminyl radical at 77 K via radiation-produced electron-mediated addition followed by N_2 removal via dissociative electron attachment mechanism and subsequent protonation from the surrounding solvent (Schemes 1 and 2).

Progressive annealing of the sample of **5** from ca. 140−160 K has resulted in the spectra (red) that are presented in Figure 4C,D (also see Figure S1). The red spectrum in Figure 4C is found to be very similar to that (blue) already reported for AmdU under equivalent conditions.[7] From the similarities (overall hyperfine splitting, the center of the spectra, and lineshape) found in the red spectra with those in the blue spectra in Figure 4B,C, the red spectra in Figure 4B,C are assigned to π-aminyl radical (U-5′-CH_2-ND·). In addition, at the right of both red and blue spectra in Figure 4B−D, the splitting of large broad resonances into three-line components is observed. This, according to our reported analysis of the AmdU sample,[7] is due to unresolved deuterium hyperfine couplings.

The broad line component found at the center of the red spectra in Figure 4B,C splits into various line components in Figure 4D as found previously for spectra (blue) of AmdU samples.[7] Following the similarities in the blue and red spectra in Figure 4D and following the assignment of these line components in the blue spectrum in Figure 4D to the C-centered α-azidoalkyl radical U-5-CH·-N_3 formed via H-abstraction by U-5-CH_2-ND· from a proximate parent, AmdU,[7] the corresponding line components at the center of the red spectrum in Figure 4E is assigned to the C-centered α-azidoalkyl radical U-5′-CH·-N_3 formed via H-abstraction by U-5′-CH_2-ND· from a proximate parent, **5** (Scheme 4).

Progressive annealing of the sample of **5** from ca. 165−170 K lead to the spectra (red) in Figure 4E,F. From the similarities of our reported spectra of AmdU samples[7] to the red spectra from **5**, it is apparent that, apart from the new line components due to

https://dx.doi.org/10.1021/acs.jpcb.0c08201
J. Phys. Chem. B XXXX, XXX, XXX−XXX

Scheme 4. Formation of Neutral π-Aminyl Radical RNH· from 5′-AZ-2′,5′-ddU (5) and 5′-AZT (6) and Its Subsequent Bimolecular Reactions with 5 or 6, Respectively[a]

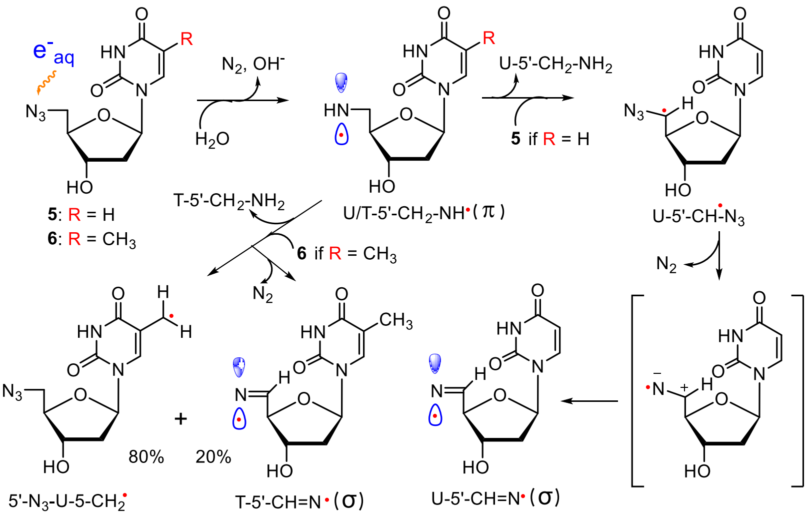

[a]H-atom abstraction from the CH_3 group at C5 in **6** by RNH· prevails (ca. 80%) in competition to the H-atom abstraction by the α-azidoalkyl radical, U-5′-CH·-N_3, from 5′-CH_2 (ca. 20%) in **6** forming the σ-iminyl radical (R═N·). As the allylic radical, U-5-CH_2·, is known to undergo either dimerization or addition to the >C═C< double bond,[4,33,34] we expect that the allylic radical from **6**, 5′-N_3-U-5-CH_2·, would undergo similar reactions. However, owing to the absence of the CH_3 group in **5**, H-atom abstraction by the α-azidoalkyl radical, U-5′-CH·-N_3, from 5′-CH_2 is the only reaction taking place, leading to the facile formation of σ-iminyl radical (R═N·).

C-centered α-azidoalkyl radical U-5′-CH·-N_3 at the center, the second species begins to be formed at the wings of the spectrum in Figure 4D and becomes the only radical whose spectra are observed in Figure 4F (see Figure S2).

The total width of the red and blue spectra in Figure 4E,F are found to be identical (ca. 155 G), and wings show line components arising from an axially symmetric anisotropic nitrogen HFCCs, $A_{\parallel}$, of ca. 36.5 G, $A_{\perp}$ = 0 and $g_{\parallel}$ = 2.0016, $g_{\perp}$ = 2.0040. The large doublet in both the red and blue spectra in Figure 4F results from a single β-proton coupling of ca. 82 G. Therefore, following our assignment to the blue spectrum in Figure 4F to the σ-iminyl radical, U-5-CH═N· from AmdU,[7] we assign the red spectrum in Figure 4F also to the σ-iminyl radical, U-5′-CH═N· (For its assignment, see Table 1 and the Supporting Information). These results show that the reactive π-U-5′-CH_2-ND·, abstracts H atom from the parent (**5**) to form the α-azidoalkyl radical intermediate, U-5′-CH·-N_3. The U-5′-CH·-N_3 promptly undergoes a unimolecular β-N_2 elimination from the azide group to produce the thermodynamically more stable σ-U-5′-CH═N· (Scheme 4 and Figure 8). Based on these assignments, we conclude that the red spectrum in Figure 4E is a cohort of spectra due to U-5′-CH·-N_3 and U-σ-5′-CH═N· whereas the cohort of spectra due to U-5-CH·-N_3 and σ-U-5-CH═N· explains the blue spectrum in Figure 4E. In addition, it is evident from these assignments that the blue spectrum in Figure 4D is a cohort of spectra due to U-5-CH_2-ND·, U-5-CH·-N_3, and σ-U-5-CH═N·.

As expected, because of the lack of an exchangeable proton at the iminyl nitrogen of U-5′-CH═N·, the EPR spectrum of this radical was the same in 7.5 M LiCl/D_2O and 7.5 M LiCl/H_2O (Figure S3) and also in 7.5 M LiBr/H_2O (Figure S4). These results add further support to our assignment of spectra in Figure 4F to the σ iminyl radical, U-5′-CH═N·. They also confirm that irrespective of solvent (D_2O or H_2O) and the glass (LiCl or LiBr), the formation of σ-U-5′-CH═N· from π-U-5′-CH_2-ND· involves the α-azidoalkyl radical intermediate, U-5′-CH·-N_3.

Studies employing samples of **5** with different concentrations (0.5 mg/mL and 5 mg/mL) showed that signal-to-noise ratios of EPR spectra increase substantially with an increase in concentration of **5** (Figure S5). These results point out that the C-centered α-azidoalkyl radical, U-5′-CH·-N_3, is formed as an intermediate via a bimolecular H-atom abstraction by π-U-5′-CH_2-ND· from a proximate **5** (Scheme 4).

Our reported work (Figures 4D and 5 in ref 8) on 5′-AZT (**6**; methylazide group at sugar) showed a small observable conversion of π-RNH· to σ-R═N· or σ-T-5′-CH═N· (ca. 20%, see Figure S6). It was shown that the H-atom abstraction reaction from the sterically accessible methyl group at C5 of thymine base by π-T-5′-CH_2-NH· predominates (ca. 80%) in **6**, leading to the formation of allylic radical, dU-CH_2· (Scheme 4). Based on our new finding of the σ-type iminyl radical spectrum from AmdU[7] and from **5**, this analysis accounts for the central multiline pattern from a superposition of the UCH_2· and T-5′-CH═N· spectra (see Figure S6). Therefore, we now conclude that this assignment corrects our earlier assignment of C3′· as the final radical spectrum to the spectra shown in Figures 4D and 5 from **6** in ref 8.

EPR investigation of the prehydrated electron attachment to 3AZPrOH (**7**), a simple model of the azido substitution at the primary carbon site, also showed σ-iminyl radical formation via the α-azidoalkyl radical intermediate (Figure S7) thereby proving the general character of the azido substitution at any primary carbon site which leads to the facile conversion of π-RNH· to σ-R═N· via the α-azidoalkyl radical intermediate.

*RNH· Formed at a Secondary Carbon Site. Nature of the Base (e.g., Cytosine in 2′-AZdC (**1**) or Uracil in 2′-AZdU (**2**)) Does Not Affect the Formation of Aminyl Radicals and Their Subsequent Reactions.* γ-Irradiation-mediated π-RNH· observed in matched homogeneous glassy samples (native pD ca. 5) of 2′-AZdU (black, **2**) and 2′-AZdC (blue, **1**) are chosen as models of π-RNH· produced at secondary carbons, and subsequent reactions of these π-RNH· are presented in Figure 5.

https://dx.doi.org/10.1021/acs.jpcb.0c08201
J. Phys. Chem. B XXXX, XXX, XXX−XXX

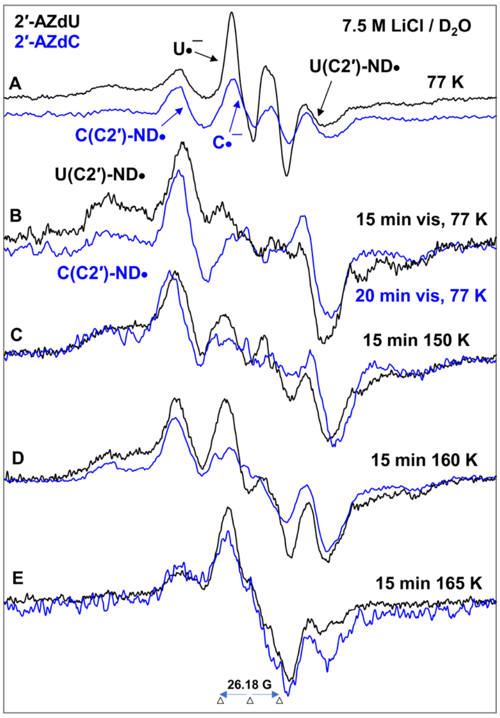

Figure 5. EPR spectra of matched samples of 2′-AZdU (**2**) (black) and 2′-AZdC (**1**) (blue) at the native pD (ca. 5) of the homogeneous glassy solution of 7.5 M LiCl in D_2O after subtraction of the $Cl_2{\cdot}^-$ spectrum[7−9,49] from the individual experimentally recorded spectrum. (A) After γ-irradiation (absorbed dose = 500 Gy) produced one-electron addition at 77 K. (B) After visible illumination of samples employing a photoflood lamp at 77 K for 15 to 20 min. The central doublet in both spectra due to the uracil anion radical ($U{\cdot}^-$) and cytosine anion radical ($C{\cdot}^-$) are removed by photoejection of the excess electron. Spectra (C)−(E) are obtained after subsequent annealing for ca. 15 min in the dark from ca. 150 to ca. 165 K. All EPR spectra shown in (A)−(E) were recorded at 77 K. See also Supporting Information, Figure S8 for additional data.

Figure 5 shows that EPR spectral characteristics (e.g., overall hyperfine splitting, *g* value at the center, and lineshape) obtained from the samples of **1** and **2** are quite identical. Hence, we conclude that the formation of π-RNH· and their subsequent reactions are similar in these samples and are not affected by the base (C (**1**) or U (**2**)).

Following spectral assignments shown in Figure 4A, the central doublets in Figure 5A are assigned to the uracil anion radical ($U{\cdot}^-$, black) and cytosine anion radical ($C{\cdot}^-$, blue).

Based on dU(C2′)-ND· assignment (Characterization of RNH· section) and on the spectral similarities observed in Figure 5A,B, the blue spectrum in Figure 5B is assigned to dC(C2′)-ND·. Therefore, dC(C2′)-ND· shows a large central doublet due to an isotropic β HFCC value of 2′-H (ca. 51.5 G), wing line component due to an axially symmetric anisotropic ^{14}N-atom HFCC (A_{zz} = 40.5 G, A_{xx} = A_{yy} = 0 G), $g_{\parallel}$ = 2.0020 and $g_{\perp}$ = 2.0043 (Characterization of RNH· section, Table 1).

Comparison of spectra in Figure 5B with those of Figure 5A shows that the central doublet owing to $U{\cdot}^-$ (black) or $C{\cdot}^-$ (blue) is absent in the spectra presented in Figure 5B. This result demonstrates that the excess electron is completely photoejected either from $U{\cdot}^-$ (black) and from $C{\cdot}^-$ (blue) via photoexcitation at 77 K and reacts with unreacted parent **1** and **2** also at 77 K to produce additional π-RNH· (dU(C2′)-ND· (or dC(C2′)-ND·)).

Based on these assignments, spectra shown in Figure 5A are found to be a cohort of $U{\cdot}^-$ (black) or $C{\cdot}^-$ (blue) (ca. 20%) and π-RNH· (dU(C2′)-ND·, black (or dC(C2′)-ND·, blue)) (ca. 80%) (see Figure 4A,B).

The spectra shown in Figure 5C−E and Figure S8 are due to subsequent reactions of dU(C2′)-ND· or dC(C2′)-ND· due to progressive annealing up to 165 K that caused softening of the glass and migration of these radicals.

The spectra presented in Figure 5E is due to the final radical formed via bimolecular reaction of either dU(C2′)-ND· (or dC(C2′)-ND·) with a proximate unreacted parent **2** or **1**. EPR spectral studies carried out using matched samples of **2** in 7.5 M LiCl/D_2O and in 7.5 M LiCl/H_2O glasses (Figure 3 (π-RNH· identification) and Figure 5E), Figure S9 (final radical spectra)) establishes that the reaction of dU(C2′)-ND· (or dC(C2′)-ND·) leads to a C-centered radical formation as there is no observable difference in the spectra in D_2O and in H_2O glasses.

There are two possible assignments of this C-centered radical. (A) The radical site could either be at the C5- or C6-site in uridine (**2**) or in cytosine (**1**) via the addition of π-RNH· (dU(C2′)-ND· or dC(C2′)-ND·) to the C6- or C5-site of the C5═C6 double bond. Alternatively, (B) π-RNH· being a good H-atom abstractor[6−9] (also, see the Introduction and Figure 4), it might cause H-atom abstraction from the 5′-site of **1** or **2** and the resulted C5′· has two possibilities: (i) it can be in a conformation, which has an anisotropic α-H coupling at C5′ and owing to a significant isotropic β-H coupling at C4′,[24] and (ii) it can undergo a ring-opening reaction leading to an open-chain conformation of C4′· (similar to our results in azidolyxofuranoside[9]) with an anisotropic α-H coupling at C4′ and owing to a significant isotropic β-H coupling at C3′.

As samples of **1** or **2** lead to similar final radical spectra (Figure 5 and Figures S8 and S9), EPR studies were performed using deuterated derivatives of **2** with deuterations at various specific positions of the sugar moiety and at the base ([**2′-D**]-**2**, [**3′-D**]-

Scheme 5. Electrophilic Addition of π-RNH· (dC(C2′)-ND·) to the C5═C6 Double Bond of the Cytosine Base in 1[a]

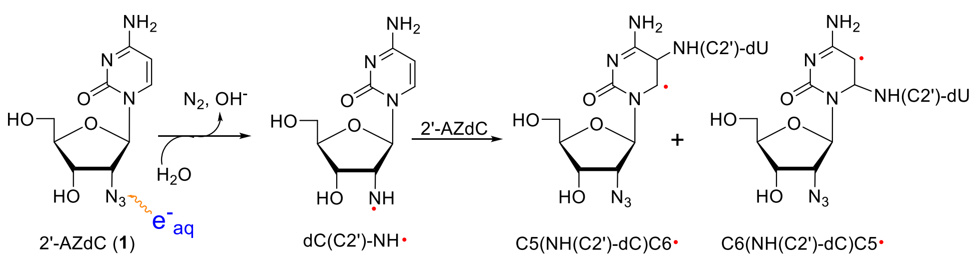

[a]The corresponding scheme for electrophilic addition of π-RNH· (dU(C2′)-ND·) to the C5═C6 double bond of the uracil base in **2** is shown in Scheme S3.

2, [4′-**D**]-**2**, and [**5,6-D,D**]-**2** (see Figure 2) to obtain an unequivocal assignment of the final radical species found in **1** or **2**. EPR spectra of non-deuterated parent **2** vis-à-vis deuterated at various positions at the sugar moiety (Figures S10 and S11) show no observable difference. These results establish that deuterations at the sugar moiety do not help in radical assignment and rule out the possibility (B) (vide supra). However, the collapse of the central part of the spectrum obtained after annealing at ca. 167 K for 1 h in the dark due to deuteration at C5 and C6 of the uracil base of **2** ([**5,6-D,D**]-**2**) (Figure S12) suggests the formation of the C-centered radical via electrophilic addition of π-RNH· (dU(C2′)-ND·) to the C5═C6 double bond of the uracil base in **2** (Scheme 5 and Scheme S1). Due to spectral similarities observed from samples of **1** and **2** (Figure 5), formation of the similar C-centered radical occurs in **1** via the same pathway (Scheme 5). These results also establish that the uracil or cytosine base does not affect the formation and subsequent reactions of π-RNH·.

*3′-Azido-2′,3′-dideoxyuridine (3′-AZ-2′,3′-ddU, **3**).* Since C3′ in the 2′-deoxyribose ring is also a secondary carbon in which the azido group can be attached, EPR studies are performed employing 3′-AZ-2′,3′-ddU, **3**; these results (black spectra) are subsequently compared with those obtained from **2** (blue spectra) and are presented in Figure 6.

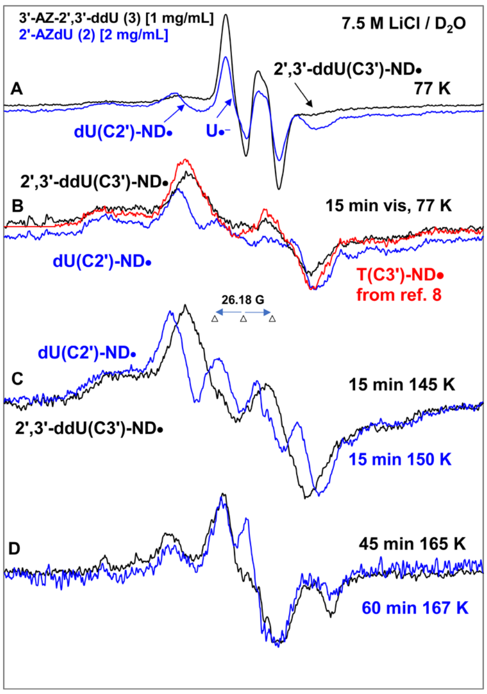

Figure 6. EPR spectra of samples of 2′-AZdU (**2**) [2 mg/mL] (blue) and 3′-AZ-2′,3′-ddU (**3**) 1 mg/mL] (black) at the native pD (ca. 5) of the homogeneous glassy solution of 7.5 M LiCl in D_2O after subtraction of the $Cl_2^{\cdot-}$ spectrum[7−9,49] from the individual experimentally recorded spectrum. (A) After γ-irradiation (absorbed dose = 500 Gy) produced one-electron addition at 77 K. (B) After visible illumination of samples employing a photoflood lamp at 77 K for 15 min. The central doublet in both spectra due to the uracil anion radical (U·$^-$) and cytosine anion radical (C·$^-$) are removed by photoejection of the excess electron. The corresponding data of the 3′-AZT sample is taken from ref 8. (C) Spectra obtained after subsequent annealing for ca. 15 min in the dark from ca. 145 to ca. 150 K. (D) Spectra obtained after subsequent annealing for ca. 45 to 60 min in the dark from ca. 165 K. All EPR spectra shown in (A)−(D) were recorded at 77 K.

Following EPR spectral results presented in Figures 4A,B and 5A,B, we assign the black 77 K spectrum presented in Figure 6A obtained after γ-irradiation as the cohort of spectra due to π-RNH· (2′,3′ddU(C3′)-ND·, ca. 80%) and U·$^-$ (ca. 20%). After 15 min photoexcitation at 77 K by a photoflood lamp, the excess electron is completely photoejected from U·$^-$, leading to only π-RNH· (2′,3′-ddU(C3′)-ND·, black spectrum in Figure 6B) similar to our findings shown in Figures 4B and 5B. As the azido group is at the 3′-site in both 3′-AZT and **3**, our reported spectrum (pink) of T(C3′)-ND· from 3′-AZT[8] is superimposed on the black spectrum of 2′,3′-ddU(C3′)-ND·. EPR characteristics (total hyperfine splitting, g value at the center, and lineshape) of these two spectra match nicely and further support our assignment of the black spectrum in Figure 6B to 2′,3′-ddU(C3′)-ND·. Therefore, β(C3′-H) HFCC, $\boldsymbol{A}_{zz}$, $\boldsymbol{A}_{xx}$, $\boldsymbol{A}_{xx}$ values of the axially symmetric anisotropic N, $g_\parallel$ and $g_\perp$ values of 2′,3′-ddU(C3′)-ND· are similar to those of T(C3′)-ND·, i.e., for 2′,3′-ddU(C3′)-ND· β(C3′-H) HFCC = ca. 41 G, $\boldsymbol{A}_{zz}$ = 37.5 G, $\boldsymbol{A}_{xx}$ = $\boldsymbol{A}_{yy}$ = 0 G, $g_\parallel$ = 2.0020 and $g_\perp$ = 2.0043.

Subsequent annealing of this sample from **3** at ca. 145 K and at ca. 165 K for 15 min in the dark led to the black spectra in Figure 6C,D. The black spectrum in Figure 6C, owing to its similarities to the black spectrum in Figure 6B, is assigned to 2′,3′-ddU(C3′)-ND·. Owing to the similarities in the blue spectra in Figure 6B,C and in Figures 6C and 5B, the blue spectrum in Figure 6C is assigned to dU(C2′)-ND· (see Figure 5).

A nice match observed between the blue and black spectra shown in Figure 6D suggests the formation of the radical species due to electrophilic addition of 2′,3′-ddU(C3′)-ND· to the C5═C6 double bond of the uracil base of a proximate parent, **3**. This reaction is similar to those observed in the case of π-RNH· formed from another secondary carbon site (2′) in **1** and **2** and their derivatives (Scheme 5 and Scheme S1).

Results presented in Figures 5 and 6 establish that, unlike azidopyrimidine nucleosides in which the azido group is attached to a primary carbon ($-CH_2N_3$) (Reactions of Aminyl Radicals section) , no observable line components due to σ-R═N· are found in azidopyrimidine nucleosides in which the azido group is attached to a secondary carbon (>CH−N_3). In addition, our earlier work on π-RNH· on a secondary carbon site (T(C3′)-ND·/T(C3′)-NH·) formed from electron addition to 3′-AZT show predominant formation of allylic UCH_2· via H-atom abstraction from the $-CH_3$ group at C5 of the thymine base.[8]

RNH· Formed at a Tertiary Carbon Site. Since the 4′-site is a tertiary carbon site in ribose (RNA) and in 2′-deoxyribose (DNA), 4′-azidocytidine (4′-AZ-C, **4**) has been chosen as the model to investigate π-RNH· formation at the tertiary carbon site and reactions of these π-RNH·. These results are compared with the formation of π-RNH· from **1** and its reactions (Figure 5). These results are presented in Figure 7.

Following EPR spectral results presented in Figures 5AB and 6A,B, we assign the black 77 K spectrum presented in Figure 7A obtained after γ-irradiation as the cohort of spectra due to π-RNH· (C(C4′)-ND·, ca. 85%) and C·$^-$ (ca. 15%). After 15 min photoexcitation at 77 K by a photoflood lamp, the excess electron is completely photoejected from C·$^-$, leading to only π-RNH· (C(C4′)-ND·, black spectrum in Figure 7B) similar to our findings shown in Figures 5B and 6B. Comparison of the black spectrum of C(C4′)-ND· presented in Figure 7B with those presented in Figures 4, 5, and 6 clearly demonstrates that C(C4′)-ND· does not have any isotropic β-H HFCC owing to the attachment of aminyl radical site N to the tertiary carbon

https://dx.doi.org/10.1021/acs.jpcb.0c08201
J. Phys. Chem. B XXXX, XXX, XXX−XXX

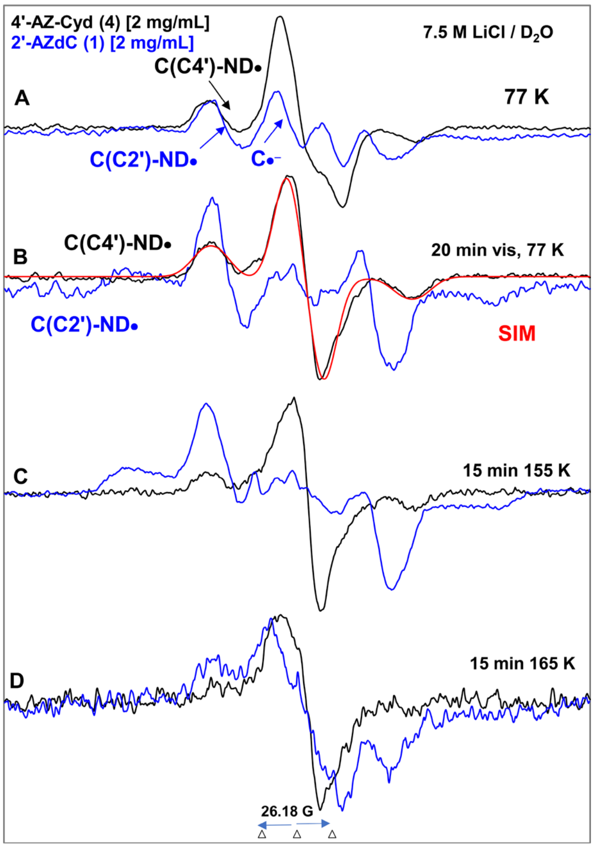

Figure 7. EPR spectra of matched samples of 4′-AZ-C (**4**, black) and 2′-AZdC (blue, **1** also shown in Figure 5) at the native pD (ca. 5) of the homogeneous glassy solution of 7.5 M LiCl in D_2O after subtraction of the $Cl_2\cdot^-$ spectrum[7−9,49] from the individual experimentally recorded spectrum. (A) After γ-irradiation (absorbed dose = 500 Gy) produced one-electron addition at 77 K. (B) After visible illumination of samples employing a photoflood lamp at 77 K for 20 min. The central doublet in both spectra due to the cytosine anion radical ($C\cdot^-$) is removed by photoejection of the excess electron. The simulated spectrum of C(C4′)-ND· is also shown (for simulation parameters, see text). Spectra (C) and (D) are obtained after subsequent annealing for 15 min in the dark at ca. 155 K and at ca. 165 K. All EPR spectra shown in (A)−(D) were recorded at 77 K.

(C4′). This spectrum has been simulated by employing axially symmetric anisotropic ^{14}N HFCC (37.5, 0, 0) G, anisotropic α-D (N-D) (4.5, 0, 6) G, a mixed Lorentzian/Gaussian (1/1) linewidth of 10 G, along with g values of (2.0020, 2.0043, 2.0043). The simulated spectrum (red) of C(C4′)-ND· obtained by employing these EPR parameters match the experimental spectrum (black) well shown in Figure 7B.

Subsequent annealing of this sample from **4** at ca. 145 K and at ca. 165 K for 15 min in the dark led to the black spectra in Figure 7C,D. The black spectrum in Figure 7C, owing to its similarities to the black spectrum in Figure 7B, is assigned to C(C4′)-ND·. The blue spectrum in Figure 7C is assigned to dC(C2′)-ND·.

The black spectrum in Figure 7D represents the decay of C(C4′)-ND·. On the other hand, the blue spectrum in Figure 7D is of the radical species due to electrophilic addition of dC(C2′)-ND· to the C5═C6 double bond of the uracil base of a proximate parent, **1** (Scheme 5). Thus, a comparison of spectra in Figure 7D suggests that π-RNH· attached to a tertiary alkyl carbon (generated from **4**) could be less reactive than π-RNH· attached to primary and secondary alkyl carbons (Scheme 6).

Scheme 6. Schematic Representation of Different Types of Reactions Undergone by π-RNH· Attached to a Primary, a Secondary, or a Tertiary Alkyl Carbon in Azidopyrimidine Nucleosides

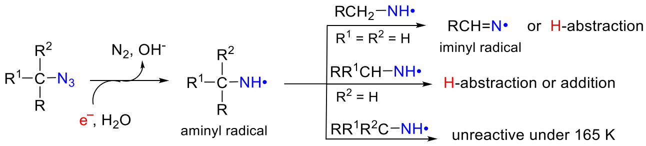

Theoretical Calculations: We have calculated the forward barrier for dissociation of the abasic 5-α-azidoalkyl radical, dR-5′-CH·-N_3, to the σ iminyl radical, dR-5′-CH═N· and N_2 in the gas phase employing dR-5′-CH·-N_3 as a model (Figure 8 and

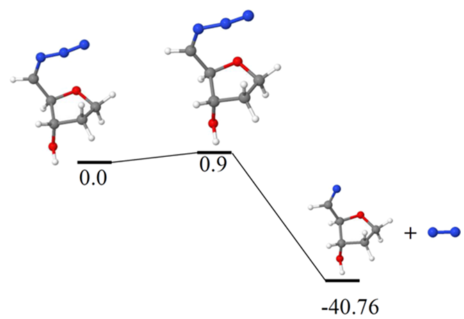

Figure 8. Dissociation of (5′-CH·)-N_3 to 5′-CH═N· and N_2 in the gas phase with a small activation barrier of only 0.9 kcal/mol. The geometries of these radicals were optimized, and relative energies (kcal/mol) were calculated by the B3LYP/6-31G** method.

Reactions of Aminyl Radicals section) to reduce the computational cost. The potential energy surface (PES) for the dissociation of dR-5′-CH·-N_3 → dR-5′-CH═N· + N_2 was calculated in the gas phase using the B3LYP/6-31G** method, see Figure 8. The relative energies (kcal/mol) of barrier height and products with respect to the reactant were calculated from the total SCF energy of each fragment shown in Figure 8. We have used the B3LYP/6-31G** optimized geometry of 5′-CH·-N_3 to obtain its HFCCs for accounting of the center of the blue spectrum in Figure 4D,E. Employing this method, we have also calculated the HFCCs of other aminyl and iminyl radicals reported in this work.

The B3LYP/6-31G** level of theory predicts a forward barrier of 0.9 kcal/mol, which is easily accessible even at the low-temperature range of our EPR experiments. The overall reaction is also predicted to be highly favorable with an energy change of −40.8 kcal/mol. The very similar EPR spectral results from samples of **5**, **6** (this work) and AmdU[7] (Figure 4 and Reactions of Aminyl Radicals section) lead us to conclude that the barriers for conversions of U-5-CH·-N_3 to σ-U-5-CH═N·, dU-5′-CH·-N_3 to σ-dU-5′-CH═N· would be similar to that calculated for dR-5′-CH·-N_3 (Table 1).

■ DISCUSSION/CONCLUSIONS

Our radiation-chemical results demonstrate the following:

(1) Unequivocal identification of aminyl and iminyl radicals: Application of ^{15}N isotopic substitution, suitable deuterations at the sugar moiety along with the collapse of the exchangeable α-N−H anisotropic HFCC by changing the solvent from H_2O to D_2O lead to the unequivocal assignment of electron-mediated site-specific formation of π-RNH·. These isotopic substitution

https://dx.doi.org/10.1021/acs.jpcb.0c08201
J. Phys. Chem. B XXXX, XXX, XXX−XXX

methods also aided the identification of subsequent radical species, e.g., iminyl radicals.

(2) Stereochemical structure and electronic environment affect the formation and reactivity of various types of π-RNH· generated from azidopyrimidine nucleosides: Despite different electronic and chemical properties π U-5′-CH_2-ND· from **5** (methylazide group in a sugar), π $HOCH_2$-CH_2-CH_2-ND· from **7** (methylazide group in an alcohol) and π U-5-CH_2-ND· from AmdU (methylazide group at the C5 position of the uracil base) have similar spectral features and undergo analogous reactions, i.e., a facile bimolecular H-atom abstraction to form α-azidoalkyl radicals, which unimolecularly and facilely convert to σ-type R═N·.

However, electron addition to the azido group attached to a secondary carbon site (2′) in **1** and **2** produces π dC(C2′)ND· and π dU(C2′)ND·, respectively, with very similar radical conformations, and these radicals undergo electrophilic addition to the C5═C6 double bond of a proximate base (C (**1**) or U (**2**)). Moreover, 2′,3′-ddU(C3′)-ND· formed via electron addition to an azido group attached to the 3′-secondary carbon site in the sugar moiety also undergoes electrophilic addition to the C5═C6 double bond of a proximate base (U (**3**)). Thus, while the azido group (and hence the π-RNH· radical) attached to a primary carbon site results in its subsequent facile conversion to σ-type R═N·, our EPR spectral results establish that these reactions are not observed in the case of the π-RNH· radical attached to a secondary carbon site (Scheme 4 vs Scheme 5), which instead undergoes ring addition. In principle, following the mechanism shown in Scheme 4, π-RNH· generated at a secondary carbon site might lead to an α-azidoalkyl radical in the sugar ring via bimolecular H-atom abstraction from a proximate unreacted parent molecule. However, restricted conformations of the cyclic ring in the transition state likely prevent the formation of iminyl radical in these cases and force the observed electrophilic addition (i.e., addition to the C5═C6 double bond) pathway.

Because of steric hindrance (i.e., due to the crowded transition state) and stabilization due to hyperconjugation, π-RNH· attached to a tertiary carbon site exhibits lower reactivity in our glassy system at low temperature. Thus, these studies provide the free radical mechanistic basis for the various types of reactions (H-atom abstraction by π-RNH· and addition of π-RNH· to the C═C double bond) that were postulated from product analyses studies by Wagner et al.[12]

(3) Implications as radiosensitizers in radiochemotherapy of cancer: Recently, π-RNH· from AmdU (π-RNH· attached to a primary carbon site) have been shown to significantly augment radiation damage in EMT6 breast cancer cells.[7] EPR spectral results presented in this work under anoxic conditions predict that π-RNH· attached to a primary or a secondary carbon site would be more effective in augmenting radiation damage to hypoxic cancer cells than π-RNH· attached to a tertiary carbon site owing to its lower reactivity. Thus, these studies have exhibited the potential to select those azidoDNA models as adjuvants that could significantly improve cancer radiotherapeutic efficacy by causing higher hypoxic cancer cell killing.

These results are of fundamental importance in the chemistry of aminyl radicals, which have widespread applications in synthesis, in environmental degradation of pharmaceuticals, in free radical-mediated damage to DNA and proteins, etc.

■ ASSOCIATED CONTENT

Supporting Information

The Supporting Information is available free of charge at https://pubs.acs.org/doi/10.1021/acs.jpcb.0c08201.

Synthetic procedures for the preparation and characterization of the deuterium labeled nucleosides and their sugar precursors (Schemes S1 and S2), additional EPR spectra (Figures S1−S12), addition of aminyl radical to uracil base in **2** (Scheme S3), and supportive theoretical calculation data (PDF)

■ AUTHOR INFORMATION

Corresponding Authors

Stanislaw F. Wnuk − *Department of Chemistry and Biochemistry, Florida International University, Miami, Florida 33199, United States;* orcid.org/0000-0002-3111-3919; Phone: 001 305 348 6195; Email: wnuk@fiu.edu; Fax: 001 305 348 3772

Amitava Adhikary − *Department of Chemistry, Oakland University, Rochester, Michigan 48309, United States;* orcid.org/0000-0001-9024-9579; Phone: 001 248 370 2094; Email: adhikary@oakland.edu; Fax: 001 248 370 2321

Authors

Mukesh Mudgal − *Department of Chemistry and Biochemistry, Florida International University, Miami, Florida 33199, United States*

Thao P. Dang − *Department of Chemistry and Biochemistry, Florida International University, Miami, Florida 33199, United States*

Adam J. Sobczak − *Department of Chemistry and Biochemistry, Florida International University, Miami, Florida 33199, United States*

Daniel A. Lumpuy − *Department of Chemistry and Biochemistry, Florida International University, Miami, Florida 33199, United States*

Priya Dutta − *Department of Chemistry, Oakland University, Rochester, Michigan 48309, United States*

Samuel Ward − *Department of Chemistry, Oakland University, Rochester, Michigan 48309, United States*

Katherine Ward − *Department of Chemistry, Oakland University, Rochester, Michigan 48309, United States*

Moaadh Alahmadi − *Department of Chemistry, Oakland University, Rochester, Michigan 48309, United States*

Anil Kumar − *Department of Chemistry, Oakland University, Rochester, Michigan 48309, United States;* orcid.org/0000-0002-9979-7798

Michael D. Sevilla − *Department of Chemistry, Oakland University, Rochester, Michigan 48309, United States;* orcid.org/0000-0001-8799-5458

Complete contact information is available at: https://pubs.acs.org/10.1021/acs.jpcb.0c08201

Notes

The authors declare no competing financial interest.

■ ACKNOWLEDGMENTS

M.D.S., A.A., and A.K. thank the National Cancer Institute of the National Institutes of Health (grant no. RO1CA045424) for support. A.A. and M.D.S. thank REF, CBR at OU for support. A.A. thanks the National Science Foundation under grant no.

CHE-1920110. T.P.D. is grateful to the FIU Graduate School for her Doctoral Evidence Acquisition fellowship and Kaufmann Foundation for support and S.F.W. to NIGMS/NCI (SC1CA138176) grant for support.

■ REFERENCES

(1) Danen, W. C.; Neugebauer, F. A. Aminyl Free Radicals. *Angew. Chem., Int. Ed.* **1975**, *14*, 783−789.

(2) Rodriguez, M. A. Light-Induced Iminyl Radicals: Generation and Synthetic Applications. In *Molecular Photochemistry: Various Aspects* InTech: 2012; pp. 265−282.

(3) Zard, S. Z. Recent Progress in the Generation and Use of Nitrogen-Centered Radicals. *Chem. Soc. Rev.* **2008**, *37*, 1603−1618.

(4) von Sonntag, C. *Free-Radical-Induced DNA Damage and Its Repair*; Springer-Verlag: Berlin, Heidelberg, 2006.

(5) Minozzi, M.; Nanni, D.; Spagnolo, P. From Azides to Nitrogen-Centered Radicals: Applications of Azide Radical Chemistry to Organic Synthesis. *Chem. − Eur. J.* **2009**, *15*, 7830−7840.

(6) Kumar, A.; Becker, D.; Adhikary, A.; Sevilla, M. D. Reaction of Electrons with DNA: Radiation Damage to Radiosensitization. *Int. J. Mol. Sci.* **2019**, *20*, 3998.

(7) Wen, Z.; Peng, J.; Tuttle, P. R.; Ren, Y.; Garcia, C.; Debnath, D.; Rishi, S.; Hanson, C.; Ward, S.; Kumar, A.; et al. Electron-mediated Aminyl and Iminyl Radicals from C5-Azido-Modified Pyrimidine Nucleosides Augment Radiation Damage to Cancer Cells. *Org. Lett.* **2018**, *20*, 7400−7404.

(8) Adhikary, A.; Khanduri, D.; Pottiboyina, V.; Rice, C. T.; Sevilla, M. D. Formation of Aminyl Radicals on Electron Attachment to AZT: Abstraction from the Sugar Phosphate Backbone versus One-Electron Oxidation of Guanine. *J. Phys. Chem. B* **2010**, *114*, 9289−9299.

(9) Mudgal, M.; Rishi, S.; Lumpuy, D. A.; Curran, K. A.; Verley, K. L.; Sobczak, A. J.; Dang, T. P.; Sulimoff, N.; Kumar, A.; Sevilla, M. D.; et al. Prehydrated One-electron Attachment to Azido-modified Pentofuranoses: Aminyl Radical Formation, Rapid H-atom Transfer and Subsequent Ring Opening. *J. Phys. Chem. B* **2017**, *121*, 4968−4980.

(10) Musa, O. M.; Horner, J. H.; Shahin, H.; Newcomb, M. A Kinetic Scale for Dialkylaminyl Radical Reactions. *J. Am. Chem. Soc.* **1996**, *118*, 3862−3868.

(11) Hwu, J. R.; Lin, C. C.; Chuang, S. H.; King, K. Y.; Su, T.-R.; Tsay, S.-C. Aminyl and Iminyl Radicals From Arylhydrazones in The Photo-induced DNA Cleavage. *Bioorg. Med. Chem.* **2004**, *12*, 2509−2515.

(12) Kuttappan-Nair, V.; Samson-Thibault, F.; Wagner, J. R. Generation of 2′-Deoxyadenosine N6-Aminyl Radicals from the Photolysis of Phenylhydrazone Derivatives. *Chem. Res. Toxicol.* **2010**, *23*, 48−54.

(13) Zheng, L.; Griesser, M.; Pratt, D. A.; Greenberg, M. M. Aminyl Radical Generation via Tandem Norrish Type I Photocleavage, β-Fragmentation: Independent Generation and Reactivity of the 2′-Deoxyadenosin-N6-yl Radical. *J. Org. Chem.* **2017**, *82*, 3571−3580.

(14) Sun, H.; Zheng, L.; Yang, K.; Greenberg, M. M. Positional Dependence of DNA Hole Transfer Efficiency in Nucleosome Core Particles. *J. Am. Chem. Soc.* **2019**, *141*, 10154−10158.

(15) Zheng, L.; Lin, L.; Qu, K.; Adhikary, A.; Sevilla, M. D.; Greenberg, M. M. Independent Photochemical Generation and Reactivity of Nitrogen-Centered Purine Nucleoside Radicals From Hydrazines. *Org. Lett.* **2017**, *19*, 6444−6447.

(16) Newcomb, M. Radical Kinetics and Clocks. In *Encyclopedia of Radicals in Chemistry, Biology and Materials*, Chatgilialoglu, C.; Studer, A., Eds. John Wiley & Sons Ltd.: Chichester, UK, 2012; pp. 107−124, DOI: 10.1002/9781119953678.rad007.

(17) Adhikary, A.; Kumar, A.; Bishop, C. T.; Wiegand, T. J.; Hindi, R. M.; Adhikary, A.; Sevilla, M. D. π-Radical to σ-Radical Tautomerization in One-Electron-Oxidized 1-Methylcytosine and Its Analogs. *J. Phys. Chem. B* **2015**, *119*, 11496−11505.

(18) Adhikary, A.; Kumar, A.; Becker, D.; Sevilla, M. D. The Guanine Cation Radical: Investigation of Deprotonation States by ESR and DFT. *J. Phys. Chem. B* **2006**, *110*, 24171−24180.

(19) Adhikary, A.; Khanduri, D.; Sevilla, M. D. Direct Observation of the Hole Protonation State and Hole Localization Site in DNA-oligomers. *J. Am. Chem. Soc.* **2009**, *131*, 8614−8619.

(20) Adhikary, A.; Kumar, A.; Munafo, S. A.; Khanduri, D.; Sevilla, M. D. Prototropic Equilibria in DNA Containing One-electron Oxidized GC: Intra-duplex *vs.* Duplex to Solvent Deprotonation. *Phys. Chem. Chem. Phys.* **2010**, *12*, 5353−5368.

(21) Adhikary, A.; Kumar, A.; Khanduri, D.; Sevilla, M. D. Effect of Base Stacking on the Acid-base Properties of the Adenine Cation Radical [$A^{\bullet+}$] in solution: ESR and DFT studies. *J. Am. Chem. Soc.* **2008**, *130*, 10282−10292.

(22) Bonifačić, M.; Armstrong, D. A.; Carmichael, I.; Asmus, K.-D. β-Fragmentation and Other Reactions Involving Aminyl Radicals from Amino Acids. *J. Phys. Chem. B* **2000**, *104*, 643−649.

(23) Bonifačić, M.; Štefanić, I.; Hug, G. L.; Armstrong, D. A.; Asmus, K.-D. Glycine Decarboxylation: The Free Radical Mechanism. *J. Am. Chem. Soc.* **1998**, *120*, 9930−9940.

(24) Adhikary, A.; Khanduri, D.; Kumar, A.; Sevilla, M. D. Photoexcitation of Adenine Cation Radical [$A^{\bullet+}$] in the Near UV-vis Region Produces Sugar Radicals in Adenosine and in Its Nucleotides. *J. Phys. Chem. B* **2008**, *112*, 15844−15855.

(25) Banyasz, A.; Ketola, T.-M.; Muñoz-Losa, A.; Rishi, S.; Adhikary, A.; Sevilla, M. D.; Martinez-Fernandez, L.; Improta, R.; Markovitsi, D. UV-Induced Adenine Radicals Induced in DNA A-Tracts: Spectral and Dynamical Characterization. *J. Phys. Chem. Lett.* **2016**, *7*, 3949−3953.

(26) Adhikary, A.; Becker, D.; Sevilla, M. D. Electron Spin Resonance of Radicals in Irradiated DNA. In *Applications of EPR in Radiation Research*; Lund, A., Shiotani, M., Eds.; Springer International Publishing: Heidelberg, New York, London, 2014; pp 299−352.

(27) Bernhard, W. A. Radical Reaction Pathways Initiated by Direct Energy Deposition in DNA by Ionizing Radiation. *Radical Radical Ion React. Nucleic Acid Chem.* **2009**, *2*, 41−68.

(28) Close, D. From the Primary Radiation Induced Radicals in DNA Constituents to Strand Breaks: Low Temperature EPR/ENDOR Studies. In *Radiation Induced Molecular Phenomena in Nucleic Acids*; Shukla, M., Leszczynski, J., Eds.; Springer: Netherlands, 2008; Vol. *5*, pp. 493−529.

(29) Sagstuen, E.; Hole, E. O. *Radiation produced radicals*; Brustolon, M., Giamello, E., Eds.; John Wiley & Sons, Inc.: NJ, 2009; pp 325−382.

(30) Steenken, S. Purine Bases, Nucleosides, and Nucleotides: Aqueous Solution Redox Chemistry and Transformation Reactions of Their Radical Cations and e− and OH Adducts. *Chem. Rev.* **1989**, *89*, 503−520.

(31) Steenken, S. Electron-Transfer-Induced Acidity/Basicity and Reactivity Changes of Purine and Pyrimidine Bases. Consequences of Redox Processes for DNA Base Pairs. *Free Radical Res. Commun.* **1992**, *16*, 349−379.

(32) O'Neill, P.; Davies, S. E. Pulse Radiolytic Study of the Interaction of $SO_4^{-\bullet}$ With Deoxynucleosides. Possible Implications for Direct Energy Deposition. *Int. J. Radiat. Biol.* **1987**, *52*, 577−587.

(33) Wagner, J. R.; Cadet, J. Oxidation Reactions of Cytosine DNA Components by Hydroxyl Radical and One-electron Oxidants in Aerated Aqueous Solutions. *Acc. Chem. Res.* **2010**, *43*, 564−571.

(34) Burrows, C. J.; Muller, J. G. Oxidative Nucleobase Modifications Leading to Strand Scission. *Chem. Rev.* **1998**, *98*, 1109−1152.

(35) Jagetia, G. C.; Aruna, R. Correlation of Micronuclei-induction With the Cell Survival in HeLa Cells Treated With A Base Analogue, Azidothymidine (AZT) Before Exposure to Different Doses of Gamma-radiation. *Toxicol. Lett.* **2003**, *139*, 33−43.

(36) Coucke, P. A.; Cottin, E.; Decosterd, L. A. Simultaneous Alteration of *De Novo* and *Salvage* Pathway to the Deoxynucleoside Triphosphate Pool by (*E*)-2′-Deoxy-(fluoromethylene)cytidine (fmdc) and Zidovudine (AZT) Results in Increased Radiosensitivity *In Vitro*. *Acta Oncol.* **2007**, *46*, 612−620.

(37) Liao, Z.-K.; Zhou, F.-X.; Luo, Z.-G.; Zhang, W.-J.; Xiong, J.; Bao, J.; Han, G.; Zhang, M.-S.; Xie, C.-H.; Zhou, Y.-F. Radio-activation of hTERT Promoter in Larynx Squamous Carcinoma Cells: An 'Indirected-activator' Strategy in Radio-gene-therapy. *Oncol. Rep.* **2008**, *19*, 281−286.

(38) Zhou, F.-X.; Liao, Z.-K.; Dai, J.; Xiong, J.; Xie, C.-H.; Luo, Z.-G.; Liu, S.-Q.; Zhou, Y.-F. Radiosensitization Effect of Zidovudine on Human Malignant Glioma Cells. *Biochem. Biophys. Res. Commun.* **2007**, *354*, 351−356.
(39) Westphal, E. M.; Blackstock, W.; Feng, W.; Israel, B.; Kenney, S. C. Activation of Lytic Epstein-Barr Virus (EBV) Infection by Radiation and Sodium Butyrate In Vitro and In Vivo: A Potential Method for Treating EBV-positive Malignancies. *Cancer Res.* **2000**, *60*, 5781−5788.
(40) van der Donk, W. A.; Stubbe, J.; Gerfen, G. J.; Bellew, B. F.; Griffin, R. G. EPR Investigations of the Inactivation of E. coli Ribonucleotide Reductase With 2′-Azido-2′-deoxyuridine 5′-Diphosphate: Evidence For the Involvement of the Thiyl Radical of C225-R1. *J. Am. Chem. Soc.* **1995**, *117*, 8908−8916.
(41) Fritscher, J.; Artin, E.; Wnuk, S.; Bar, G.; Robblee, J. H.; Kacprzak, S.; Kaupp, M.; Griffin, R. G.; Bennati, M.; Stubbe, J. Structure of the Nitrogen-Centered Radical Formed During Inactivation of E. coli Ribonucleotide Reductase by 2′-Azido-2′-deoxyuridine-5′-diphosphate: Trapping of the 3'-Ketonucleotide. *J. Am. Chem. Soc.* **2005**, *127*, 7729−7738.
(42) Wnuk, S. F.; Mudgal, M. M.; Nowak, I.; Robins, M. J. Model Substrate/Inactivation Reactions for MoaA and Ribonucleotide Reductases: Loss of Bromo, Chloro, or Tosylate Groups from C2 of 1,5-Dideoxyhomoribofuranoses upon Generation of an α-Oxy Radical at C3. *Molecules* **2020**, *25*, 2539−2561.
(43) Fauster, K.; Hartl, M.; Santner, T.; Aigner, M.; Kreutz, C.; Bister, K.; Ennifar, E.; Micura, R. 2′-Azido RNA, A Versatile Tool for Chemical Biology: Synthesis, X-ray Structure, siRNA Applications, Click Labeling. *ACS Chem. Biol.* **2012**, *7*, 581−589.
(44) Maag, H.; Rydzewski, R. M.; McRoberts, M. J.; Crawford-Ruth, D.; Verheyden, J. P. H.; Prisbe, E. J. Synthesis and Anti-HIV Activity of 4′-Azido- and 4′-Methoxynucleosides. *J. Med. Chem.* **1992**, *35*, 1440−1451.
(45) Hampton, A.; Nichol, A. W. Nucleotides. V. Purine Ribonucleoside 2′,3'-Cyclic Carbonates. Preparation and Use for the Synthesis of 5'-Monosubstituted Nucleosides. *Biochemistry* **1966**, *5*, 2076−2082.
(46) Wnuk, S. F.; Chowdhury, S. M.; Garcia, P. I.; Robins, M. J. Stereo-defined Synthesis of O3'-Labeled Uracil Nucleosides. 3'-[^{17}O]-2′-Azido-2′-deoxyuridine 5′-Diphosphate as a Probe for the Mechanism of Inactivation of Ribonucleotide Reductases. *J. Org. Chem.* **2002**, *67*, 1816−1819.
(47) Li, H.; Jiang, Z.; Wang, X.; Zheng, C. Synthesis of 2′-Amino-2′-deoxyuridine Modified by 1,8-Naphthalimide. *Synth. Commun.* **2006**, *36*, 1933−1940.
(48) Gai, X. S.; Fenlon, E. E.; Brewer, S. H. A Sensitive Multispectroscopic Probe for Nucleic Acids. *J. Phys. Chem. B* **2010**, *114*, 7958−7966.
(49) Khanduri, D.; Adhikary, A.; Sevilla, M. D. Highly Oxidizing Excited States of One-Electron-Oxidized Guanine in DNA: Wavelength and pH Dependence. *J. Am. Chem. Soc.* **2011**, *133*, 4527−4537.
(50) Petrovici, A.; Adhikary, A.; Kumar, A.; Sevilla, M. Presolvated Electron Reaction with Methylacetoacetate: Electron Localization, Proton-Deuteron Exchange, and H-atom Abstraction. *Molecules* **2014**, *19*, 13486−13497.
(51) Kaczmarek, R.; Ward, S.; Debnath, D.; Jacobs, T.; Stark, A. D.; Korczyński, D.; Kumar, A.; Sevilla, M.; Denisov, S. A.; Shcherbakov, V.; et al. One Way Traffic: Base-to-backbone Hole Transfer in Nucleoside Phosphorodithioates. *Chem. − Eur. J.* **2020**, *26*, 9495−9505.
(52) McDonald, R. N.; Chowdhury, A. K.; Setser, D. W. Gas-Phase Generation of Phenylnitrene Anion Radical-Proton Affinity and ΔH_f° of $PhN^{-\bullet}$ and Its Clustering with ROH Molecules. *J. Am. Chem. Soc.* **1981**, *103*, 6599−6603.
(53) Živanov, S.; Ibanescu, B. C.; Paech, M.; Poffet, M.; Baettig, P.; Sergenton, A.-C.; Grimme, S.; Allan, M. Dissociative Electron Attachment and Electron Energy-loss Spectra of Phenyl Azide. *J. Phys. B: At., Mol. Opt. Phys.* **2007**, *40*, 101−109.
(54) Warrier, M.; Lo, M. K. F.; Monbouquette, H.; Garcia-Garibay, M. A. Photocatalytic reduction of aromatic azides to amines using CdS and CdSe nanoparticles. *Photochem. Photobiol. Sci.* **2004**, *3*, 859−863.
(55) Joshi, R.; Adhikari, S.; Mukherjee, T. Redox reactions of 3′-azido-3′-deoxythymidine (AZT) and interaction of its ·OH-derived radical with bilirubin and riboflavin: A pulse radiolysis study. *Res. Chem. Intermed.* **2001**, *27*, 623−634.